SEASONAL DISTRIBUTION OF FE, MN AND ZN IN SEDIMENT TRAPS AND SUSPENDED PARTICLES IN RESPONSE TO ATMOSPHERIC INPUT TO THE SARGASSO SEA

by

Amanda Rae Vandermark

A thesis submitted to the Faculty of the University of Delaware in partial fulfillment of the requirements for the degree of Master of Science in Marine Studies

Summer 2011

SEASONAL DISTRIBUTION OF FE, MN AND ZN IN SEDIMENT TRAPS AND SUSPENDED PARTICLES IN RESPONSE TO ATMOSPHERIC INPUT TO THE SARGASSO SEA

by
Amanda Rae Vandermark

Approved: _____
Thomas M. Church, Ph.D.
Professor in charge of thesis on behalf of the Advisory Committee

Approved: _____
Charles E. Epifanio, Ph.D.
Director of the School of Marine Science and Policy

Approved: _____
Nancy M. Targett, Ph.D.
Dean of the College of Earth, Ocean, and Environment

Approved: _____
Charles G. Riordan, Ph.D.
Vice Provost for Graduate and Professional Education

ACKNOWLEDGMENTS

I am grateful for the experiences I've had while furthering my education through this institution. Although this pursuit was not unique, in the trying endeavors of a graduate student, I feel that I am graduating with new skills and life lessons that will enrich my life hereafter. For this I have many to thank.

Thank you, Dr. Church, for always putting me up to new challenges as well as providing me with opportunities to learn techniques at BIOS and FSU that would help me with my research. Thank you, Simon, for your encouragement, guidance and easy going but efficient approach to research. Thank you, Dr. Luther, for your ideas and valuable insight on trace metal chemistry. To my lab mate, Maria, thank you for your friendship these past few years- a balance of sharing life's highs and a little empathizing here and there. Lastly, I am indebted to my parents, my brother and my boyfriend, whom all continue to support and love me unconditionally.

This research was funded by the NSF as well as the Delaware EPSCoR. Special thanks to Caroline Golt, for ICPMS analysis. I would like to acknowledge Maureen Conte for her work with the sediment trap samples and kindly sharing supplementary data for this study. I would also like to acknowledge Zhenglong Tian and colleagues, who performed the initial GFAAS analysis on the trap digestions and atmospheric samples.

TABLE OF CONTENTS

LIST OF TABLES

LIST OF FIGURES

ABSTRACT

Matching atmospheric samples (bulk and wet) and water column samples (sediment trap and suspended particles) were collected from July 1999 through April 2000, at the AEROCE tower and OFP Mooring Site in the Sargasso Sea. Using a 'top-down' approach, seasonal variability of the atmospheric input of Fe, Mn and Zn, and the subsequent processing in the water column in the surface, mid-water and deep-waters were investigated. Variability in mass flux at the 500 m, 1500 m, and 3200 m traps highlighted seasonal abiotic and biotic processes. The presence of salp fecal pellets in the sediment traps collected during the summer are thought to have rapidly processed atmospheric input in the surface ocean, supported by the coupling of increased input and output flux observed during that time. Increased winter mixing observed in temperature profiles in December indicates that aggregation and scavenging of surface particles. The increase in mass flux at all trap depths during April is supported by the sinking of aggregated phytoplankton from the spring bloom and subsequent grazing by zooplankton.

Residence times for Fe, Mn and Zn in the 'total' reservoir (dissolved seawater and suspended particles) were calculated at different depth intervals corresponding to the mixed layer depth during the summer/fall, fall/winter and winter/spring. The input flux (soluble wet + soluble calculated dry) was compared with the output flux (500 m trap), in which variable residence times resulted. Fe ranged from 8- 140 d when calculating residence

time using the input flux, and 0.4- 1.3 d range when using output flux, Mn ranged from 1- 60 d using input flux and 30- 184d using output flux and Zn ranged from 2- 36 d using input flux and 7- 16 d when using output flux. Residence times for Fe when using input fluxes agreed with literature values in surface waters. However, the residence times for Mn when using output flux were closer to literature values but were still much shorter.

The lithogenic to biogenic component of the trace elements in trap particles and suspended particles were related to the loss of organic carbon with depth, with results in agreement to calculations with trap data from. Biogenic Zn decreased with depth in trap particles but increased in suspended particles. For Fe, the biogenic to organic carbon ratio both increase in addition to the lithogenic component. Results indicated the presence of Mn-oxides on particles with depth, in which there was an increase in the biogenic component of Mn and an increase in the lithogenic component of Fe through scavenging. Stoichiometric ratios of the surface most suspended particles collected in January (20 m) and May (50 m) revealed biotic and abiotic influence and a ratio comparable to ratios reported for phytoplankton composition (C1000Fe0.10Mn0.0035Zn0.005). Overall this investigation supports the relationship between trace element cycles and the influence of biotic and abiotic processing that impact the distribution in the water column.

Chapter 1

BACKGROUND

Trace elements play a variety of roles in marine environments. Under certain concentrations they are beneficial and sustain life, while on the other hand they can form detrimental compounds with toxic effects when in excess. The resulting biological activity and impact on the environment depends heavily on the physico-chemical forms of these metals, which dictates bioavailability.

Trace metal analysis has been focused mainly on Fe, in response to the direct impact it has on primary production (Martin et al., 1994). It is now better understood that trace metals, such as Mn and Zn, play an essential role in primary production and metabolic processes of aquatic life as well (Morel and Price, 2003). Photosynthetic processes require these elements in addition to sunlight, proper pigmentation, nitrogen, and phosphorus (Hunter et al., 1997). Continued efforts are necessary to expand current knowledge of the utilization and cycling of bioessential trace metals.

1.1 Seasonal Cycle and Atmospheric Deposition to the Surface Ocean

Upper ocean seasonal cycles in the Bermuda region span three months (Huang et al., 1999) and play a large role in the level of primary production that can be sustained. Spring is defined as March until May,

summer is defined as May through August, fall is defined as September until November, and winter is defined as December until February. During the winter into the early spring, there are relatively high levels of primary production, whereas low levels are generally observed from late spring to early fall (Menzel and Ryther, 1960). Short spring blooms are associated with rapid recycling of available nutrients and vertical winter mixing ranging to depths from 150 m to 300 m (Steinberg et al., 2001), closer to the permanent thermocline at roughly 400 m (Menzel and Ryther, 1960). On the other hand, low levels typically involve a highly stratified water column with a thermocline in the upper 100 m (Steinberg et al., 2001). With the lack of available nutrients, phytoplankton growth and production is slowed down. Although this is the general trend for the seasonality of this region of the Sargasso Sea, physical processes within the subtropical gyre, such as eddies, can cause distinct variability in trace metal transport from year to year (Huang and Conte, 2009).

Seasonal changes are also significant in that air parcel trajectories originate from different sources during the year. Dust events to Bermuda originate predominately from the Sahara (Tian et al., 2008). However, from late fall through early spring, dusts from North America are more typical (Chen and Duce, 1983). Each type of dust is present in different chemical forms as they are delivered to the surface Sargasso Sea. Saharan dusts are much finer particles due to extended weathering that occurs during transit (Bory et al., 2002). Many of these particles are scavenged by rain because of the decrease in gravitational deposition. Dusts that have a shorter distance to

travel, like dusts from North America, are influenced relatively less by atmospheric processing and therefore are deposited as larger, coarser particles.

The dusts that are scavenged into the cloud processing system, and undergo condensation/evaporation processing cycles can form metal aggregates that appear to be more bioactive (Shi et al., 2009). Generally during transport, one particle will typically undergo at least ten condensation/evaporation cycles, consisting of changes that occur from chemical and physical weathering (Desboeufs et al., 2001). The degree to which the solubility of the particle will be modified depends on the metal and its characterization. Introduced as either aerosols or by precipitation, the origin influences the solubility of these elements and in turn influences the bioavailability and overall distribution in the water column (Tian et al., 2008).

The impact of processing is evident upon the mixing of rainwater and seawater, in which waters from an acidic, fresh-water environment are introduced into an alkaline, saline environment. Before uptake and utilization can occur, the metal must be present in a form that is bioavailable. The speciation of the deposited metal impacts the degree of solubility, bioavailability, adsorption, residence time onto particles, as well as the redox behavior within the water column (Desboeufs et al., 2001).

Although little is known about the role of the surface micro-layer in the chemical dynamics of rainwater and seawater mixing, it seems to have significant impact in the aquatic behavior of metals (Church and Jickells, 2008). Although the surface layer is only a few millimeters in thickness, it is an

enriched environment with organics, including colloids and surfactants. The organic nature of the surface microlayer may contribute to complexation or formation of colloids. Colloidal iron has been found to incorporate a large fraction of iron in the ocean that was previously defined as ‘dissolved’. At the surface of the Sargasso Sea, colloidal iron can be more abundant compared to the upper nutricline. Soluble iron on the other hand shows the opposite distribution (Wu et al., 2001).

1.2 Vertical Distribution and Biological Impact

Considering the vertical profile from atmosphere down the water column, depth categories have characteristic chemical and biological behavior that influences the distribution of elements. The slow mixing of bottom waters to advect metals and nutrients to shallower depths, suggests that biological processing has a large impact on the distribution on the surface ocean. This is evident by the surface bio-limiting profiles that have been observed for most bioessential elements. The bioessential trace metals of discussion, except for Mn, typically have concentration profiles that are depleted at the surface, due to uptake and grazing (Morel and Price, 2003). The surface enrichment for Mn is attributed to atmospheric deposition and the extensive redox cycling that takes place in the upper water column (Bruland et al., 1991). Other processes that impact the distributions at the surface include aggregation, precipitation, and scavenging (Huang and Conte, 2009).

Previous studies have speculated that the majority of bioessential metals in surface waters are present in a speciation and is not bioavailable (Morel and Price, 2003). In response, there are organisms that have adapted

by manipulating the speciation of the elements they require. One line of evidence for this is the production of biogenically generated ligands used to complex trace metals and their high concentration in the euphotic zone (Bruland et al., 1991). Some organisms are able to release extracellular chelators that are metal specific (Vraspir and Butler, 2009). For example, siderophores bind iron to facilitate the uptake into the organism for further processing (Butler, 2005). Other organisms, however, release biogenic ligands can also be used to limit the potential toxicity of elements, as in the case for Cu-sensitive phytoplankton (Moffett and Brand, 1996). In this case, complexing the metal inhibits uptake by making the metal less bioavailable. Depending on requirement of bioessential elements individually or in relation to other organisms, the distribution in the water column will be impacted by biological processes (Maldonado et al., 2006).

In open-ocean locations where trace elements are scarce, the demand of organism for these elements further influences the availability of the element. Depending on the enzymatic requirements of the organism, processes such as uptake, bioaccumulation, excretion as particulate matter, and remineralization occur at different rates. For instance, Cd has been found to be recycled faster than any other element whereas Zn appears to be retained longer in the organism, as illustrated by the typically low flux in open water (Whitfield, 2001). Clearly, in an environment where the bioessential elements needed for life are scarce, it is necessary for organisms in surface waters to be resourceful and have the ability to recycle materials.

1.3 The Role of Bioactive Elements in Marine Organisms

In certain cases, it has been found that bioactive metals will substitute for each other if there is a limitation of one metal. For instance, diatoms do not necessarily discriminate between Co, Cd, and Zn, as they have been found to be functionally interchangeable (Lane et al., 2005). For example, depending on conditions and availability, phytoplankton can utilize Fe, Mn, Cu and Zn, and Ni in superoxide dismutase (Morel, 2008). This enzyme in particular protects the cell from oxidative damage caused by oxygen radicals. In other species it is also possible that an enzyme utilizes multiple metals to function properly. The possibility of substitution under limited conditions supports the ideas of the adaptability of primary producers to the changing chemistry of the oceans over time (Glass et al., 2009). By becoming familiar with the known functions carried out by the metals for certain enzymatic processes, it helps to understand the relative ratios needed within the organism.

Bioessential elements play a significant role in the pursuits of an organism to fulfill fundamental conditions of life, including self-replication and the selective catalysis of chemical reactions (Nelson and Cox, 2005). These biochemical processes require specific enzymes, which further have their own requirements for proper function. Enzymatic activity is highly catalytic under the proper temperature, pH, and saline conditions, which accelerate biochemical reactions within an organism. Nearly all enzymes are proteins, having a specialized function that is dictated by its structure. Some enzymes are metalloenzymes which require a metal ion as a coenzyme. Coenzymes can consist of one or more inorganic ions or a metallo-oganic molecule.

Typically, the function of coenzymes is to assist the transfer of specific functional groups through oxidation reduction reactions (Nelson and Cox, 2005).

In the environment, bioessential metals including Fe, Cd, Cu, Mn, Ni, and Zn can be found in the cationic form as well as complexed, and act as coenzymes for essential biochemical processes. Proper function of the enzyme is dependent on specific ionic interactions with these cations (Nelson and Cox, 2005). For example, some coenzymes are involved in ion interactions that help to orient the substrate, in which the specific orientation is crucial for catalysis to occur. Other coenzymes are located in a position within the enzyme that allows them to stabilize the intermediate during the reaction. Coenzymes in some enzymes undergo reversible changes of their oxidation state to regulate oxidation-reduction reactions. In all of these cases, it is structure of the enzyme with cofactor that dictates its function. Examples of bioessential ion cofactors and associated enzyme within marine organisms are shown in Table 1.

Table 1. Suite of bioactive trace metals and some corresponding enzymes found in marine phytoplankton (from Morel and Price, 2003). * from Sunda (2000)

Trace Metal Coenzyme	Metalloenzyme
Fe	nitrogenase, nitrate reductase, nitrite reductase
Zn	carbonic anhydrase, alkaline phosphatase
*Mn	photosystem II

The uptake of bioactive metals by an organism is a carefully regulated and competitive process. Specialized proteins embedded in the cellular membrane facilitate transport of metal ions upon binding. In particular, some transport proteins are specific for one metal, depending on the metal and requirement by the organism like Co for growth as vitamin-B12 (Sunda, 2000). A combination of reactions occurs at the transport site including redox, complexation, oxide dissolution, as well as ligand-exchange reactions (Sunda, 1989). Regulation of uptake also depends on the potential levels of growth and metabolism if conditions were optimized. For some metals this utilizes high and low affinity systems, sometimes with negative feedback in resource limited conditions (Sunda, 2000). For instance, the affinity constant for manganese in phytoplankton is fixed whereas the maximum uptake rate is regulated. When the external environment of a phytoplankton is depleted of available Mn, the maximum uptake rate increases maintain the internal concentration of manganese. When the external concentration is decreased low enough, the maximum uptake rate reaches a point where it can no longer be increased. At this point, growth rate decreases because concentrations to the phytoplankton are no longer adequate to support primary production.

Overall, as integral components of the physiology of phytoplankton and other marine organisms, individual bioessential trace metals play specific roles in enzymatic processes. Iron is essential for enzymatic processes including chlorophyll production in phytoplankton and nitrogen assimilation in marine life such as in trichodesmium (Achilles et al., 2003). Manganese can be utilized as a cofactor in Mn-superoxide dismutase, although it can be

substituted for other available metals. In marine phytoplankton manganese is necessary for photosynthesis to occur and is utilized in the oxidation of water (Sunda, 2000). In overall biogeochemical processes manganese serves in the fixation of carbon (Morel and Price, 2003).

Zinc is less available, as it is only present in the +2 oxidation state (Sunda, 2000). Biochemically it plays a role in hydrolytic reactions, behaving as a Lewis acid. Important processes such as DNA replication as well as mitosis utilize zinc to work efficiently. In alkaline phosphatase, zinc is the coenzyme needed to obtain and utilize organic phosphorous in the available form (Shaked et al., 2006). Under Zn limited conditions, for example, the regeneration of phosphorous becomes limited. Furthermore, a Zn-P colimitation is suggested to occur during phytoplankton blooms in oligotrophic waters, such as the Sargasso Sea. Other important processes in the biogeochemical cycle of Zn include: the fixation of CO_2, the uptake of silica for the formation of diatom frustules, and in the remineralization of other materials (Morel and Price, 2003).

1.4 Ocean Flux Program (OFP) and Sediment Traps

The Oceanic Flux Program (OFP) time-series provides a record for seasonal biotic and abiotic fluxes of trace metals in sediment traps (Huang and Conte, 2009). This program establishes a link between these fluxes and provides a means to investigate productivity of the upper ocean through the comparison with other sample types. Sediment traps deployed at the OFP mooring site, located at 31˚ 50’N, 64 ˚ 10’W, targets three depth regions. The first trap is positioned at 500 m, beneath the photic zone and seasonal

thermocline, and collects repackaged material associated with biological processing in the surface waters. Rapid remineralization of organic matter takes place at the surface, supporting the recycling of trace metals (Morel and Price, 2003). The second trap, at 1500 m, collects downward fluxing particles between the mesopelagic to bathypelagic zone. In this region, further processing of the particles occur including: aggregation of particulate matter, remineralization and scavenging (Huang and Conte, 2009). In addition, further contribution to the downward flux by zooplankton continues, through processes such as vertical migration (Turner, 2002). The third trap is located at 3200 m, capturing large particles descending between the bathypelagic to abyssalpelagic zone. These particles are in transit to the benthos to be buried or later recycled and advected to upper layers.

In the past it was thought that the material collected in sediment traps was primarily fecal pellets from zooplankton. However, it is now better understood that organic aggregates also contribute to the downward flux of particles. At times this contribution is more substantial than large zooplankton fecal pellets (Turner, 2002). Specifically, organic aggregates in this case refer to ‘marine snow’ and sinking phytoplankton blooms. Many variables influence these three sinking components, such as size, sinking rates, locations and depths. In addition, each component should be considered as related and integrated with the other components. For instance, fecal pellets can scavenge marine snow. At the same time small fecal pellets can contribute to the reservoir of marine snow.

Fragmented food particles that remain in the water column share the same potential fate as incoming particles. They can be adsorbed and become incorporated into sinking particles, scavenged by nearby aggregates, slowly released as organic matter decomposes from the microbial activity within the environment of the aggregate, or further processed biotically (Huang and Conte, 2009). The food particles that are consumed enter a microenvironment within the gut where the elements can desorb from particulate matter to either bioaccumulate or become utilized biochemically. Lastly, elements that are not utilized by the organism will be repackaged and released in the form of a fecal pellet or mucous structure. Fluxes of repackaged biomass settle down the water column, with remineralization of trace elements at lower depths (Morel and Price, 2003).

There is variability in the sinking rate of fecal pellets and organic aggregates (Turner, 2002). Phytodetrius has an estimated sinking rate of 100-150 m d^{-1}, whereas marine snow sinks at a rate of 16-368 m d^{-1}. Zooplankters, such as copepods and salps have a sinking rate of 5-220 m d^{-1} and 43-2700 m d^{-1}. Copepods are very abundant in the surface depths of the Sargasso Sea and account for 75-85% of mesozooplankton (Andersen et al., 2011). However, other zooplankton such as dinoflagellates and ciliates are more efficient grazers. Large fecal pellets would have the fastest sinking velocity, therefore would be less affected by decomposition by microbes in transit to the benthos (Turner et al., 2002). On the other hand, smaller fecal pellets from micro-zooplankton are thoroughly processed and contribute to upper ocean processes by being recycled in the water column.

The dominate source of organic material from the epipelagic to the abyssal zone has been found to be due to the sinking of aggregated phytoplankton, providing nourishment for deep sea organisms (Turner et al., 2002). This is supported in Conte et al. (2003), in which a phytoplankton bloom at the Bermuda Atlantic Time Series (BATS) site was observed followed by a pulse of organic material in the deep ocean trap at 3200 m. The variation of downward fluxing particles, whether as repackaged material, suspended particles or unconsumed phytoplankton couple production at the surface with deep-ocean processes. Overall, the distribution of trace metals throughout the water column are heavily impacted by the downward flux of large particles (Santschi, 1984). This ability to link oceanic processes throughout the different regions within the water column achieves one of the goals of the OFP program (Huang and Conte, 2009).

Chapter 2

SEASONAL DISTRIBUTION OF FE, MN, AND ZN IN SEDIMENT TRAPS AND SUSPENDED PARTICLES IN REPSONSE TO ATMOSPHERIC INPUT TO THE SARGASSO SEA

2.1 Introduction

Trace elements play a large role in the metabolic processes of marine life. Iron has been the dominant focus of trace metal research, as it was found to stimulate primary production (Martin et al., 1994). However, additional trace metals are essential to aquatic life as well. Over the past two decades, it has become better understood that trace metals such as Mn and Zn, in addition to Fe, are required for metabolic processes such as photosynthesis (Morel and Price, 2003). Current investigations are uncovering further complexities of the biogeochemical cycles of these essential metals and the factors that control their distribution in the water column.

Atmospheric deposition is a major source of essential trace metals to the surface open ocean, with aerosol origins often varying seasonally (Tian et al., 2008). Dust events to Bermuda originate predominantly from the Sahara. However, from late fall through early spring, dusts from North America are more common (Chen and Duce, 1983). Although the source of Fe and Mn is predominately crustal, both have been found to have anthropogenic origins as well (Church et al., 1984). On the other hand, atmospheric Zn is mostly anthropogenic in origin. Whether introduced as

aerosols or by precipitation, the source of these metals influences their bioavailability and in turn influences their overall distribution in the water column (Maldonado et al., 2006).

The Oceanic Flux Program (OFP) time-series provides a record of seasonal biotic and abiotic fluxes of trace metals in sediment traps deployed at the surface, mid-water, and deep ocean (Huang and Conte, 2009) in the Bermuda Atlantic Time Series (BATS) region. In addition, the OFP establishes a link among these fluxes and presents a means to investigate the productivity of the upper ocean through comparison with other sample types, including atmospheric input. The variation of downward fluxing particles, whether as repackaged material, suspended particles or unconsumed phytoplankton couple production at the surface with deep-ocean processes. Overall, the distribution of trace metals throughout the water column are heavily impacted by the downward flux of large particles (Santschi, 1984). The OFP program provides the opportunity to link oceanic processes throughout the different regions within the water column (Huang and Conte, 2009).

Even as Fe, Mn and Zn are essential for marine life, limited data exists on the atmospheric delivery and cycling of these metals in the surface ocean and with depth. In particular few studies have focused on the processing that occurs in the upper 500 m. In the Sargasso Sea, the contribution of the suspended particle pool to a suite of trace metals to the downward flux at the 3200 m trap has been reported (Sherrell and Boyle 1992). In the Baltic Sea, the vertical distribution of the dissolved and particulate profiles of trace elements was investigation in surface waters from

December 1999 to February 2001 (Pohl et al., 2004). Several studies have investigated seasonal variation of bioessential elements in atmospheric flux, but only with comparison to a 3200 m trap (Conte et al., 2001; Kuss et al., 2010; Sherrell and Boyle, 1992). A comparison between complementary samples from the atmosphere, sediment trap, suspended particle, and dissolved fraction has not yet been examined in the Sargasso Sea. It is the utilization of synchronous samples that provide for a better understanding of how both the larger and smaller oceanic processes work together.

Our goal was to investigate the fate and processing of Fe, Mn and Zn from atmospheric input to the surface ocean through the water column by biotic and non-biotic means. To achieve this goal, we determined the distribution of trace elements in downward fluxing trap particles (500-1000µm), small suspended particles (>0.45µm) and compare this to existing atmospheric and filtered seawater profiles. We calculate seasonal residence times based on atmospheric input versus output at the 500 m trap as well as the dissolved and particulate reservoirs. The particle and dissolved reservoirs from the mixed layer during three seasons reflect the processing that occurs in the photic zone. We identify the lithogenic and biogenic component in trap sediments and suspended particles, calculate biogenic metal to organic carbon ratios for each sample, and provide a stoichiometric ratio for suspended particles. Calculations are repeated with data reported in other studies to compare our findings. External databases and records were used to further interpret our data. Overall, these data contribute to the growing understanding of the overall biogeochemical cycling of Fe, Mn and Zn.

Through this study we hope to contribute data on the biotic and abiotic influences on seasonal input and trace metal cycling.

2.2 Materials and Methods

2.2.1 Sample Collection

Atmospheric samples (bulk and wet) were collected at the AEROCE tower located on Tudor Hill, on the Southwest coast of Bermuda (Fig. 1). The sampling protocol followed for atmospheric collection can be found in Kim et al, (1999). Both bulk and wet deposition were collected on the AEROCE tower from July 1999 to April 2000. Bulk refers to the open collection apparatus in which both wet and dry input are collected. The wet component (rain) was collected using an automatic rain sampler. The wet value was subtracted from the bulk value to calculate the dry component of atmospheric input.

Samples including sediment traps and suspended particles were collected as part of Ocean Flux Program (OFP) cruises during September ’99, January ’00 and May ’00 (Fig. 1). Trap particles were collected biweekly from July 1999 to April 2000 at 500m, 1500m and 3200m. The protocols for deployment, collection, and splitting of the sediment trap samples have been documented (Conte et al., 2001). Well established trace metal-clean equipment was deployed (Huang and Conte, 2009). Suspended particles profiles were collected during January 2000 and May 2000. A modified McLane pump (trace metal- clean) was used to pump 50-1000L of seawater over filters (0.45 µm pore size, Supor) at five depths. During January,

suspended particles were samples at 20m, 70m, 120m, 450m and 3150m. Suspended particles for May were sampled at 50m, 100m, 550m, 1550m, and 3250m.

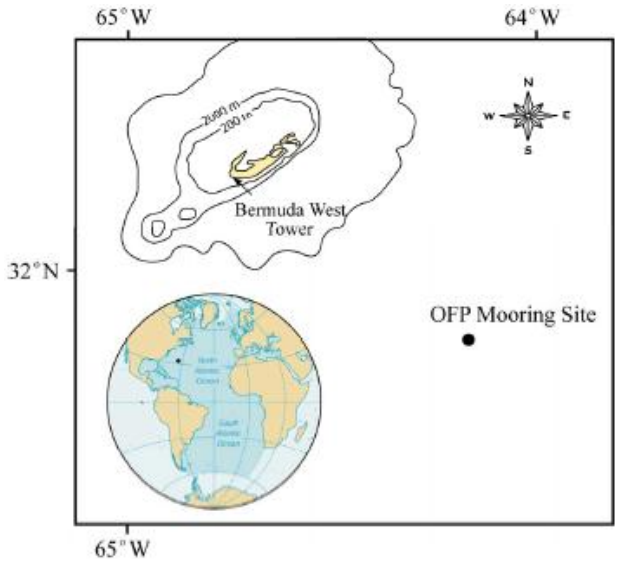

Figure 1. Sampling sites for atmospheric and Sargasso Sea samples. Wet deposition and bulk samples were collected on the Bermuda West Tower (AEROCE Tower). Trap particles and suspended particles were collected offshore at the Ocean Flux Program (OFP) Mooring Site.

2.2.2 Processing and Analysis

All analytical work was performed under clean room conditions. To further reduce the risk of contamination, samples were digested in a Class-100 Laminar flow hood designated for acid use. Digestion vials (Savillex- 15 ml) were preconditioned through a series of acid baths: 40% HNO_3, 15% HNO_3, 10% HCl, and 0.5% HCl. Sample bottles (PTFE) were preconditioned

through the following baths: 15% HNO_3, 10% HCl, and 0.5% HCl. All materials were rinsed thoroughly with quartz distilled water following the last bath.

Subsamples of suspended particle filters (0.45 µm Supor) were digested using a modified digestion procedure from Tian et al, (2008). A diluted acid mixture was used, consisting of quartz distilled H_2O, HNO_3 and HCl, and concentrated HF in a 4:3:2:1 ratio. The resulting normalities of the acid components were as follows: 5.1 N HNO_3, 1.2 N HCl, and 2.26 N HF. One fourth to one eighth filter aliquots were transferred gravimetrically to tared vials. Approximately 2 ml of the acid mixture were added to each sample. The vials were capped and heated at 140-150˚C overnight. Uncapped, the digestate was evaporated to near dryness, and a second portion of 2 ml acid solution was added. The vials were recapped and heated overnight. The filters were removed from the vials and were rinsed with quartz distilled H_2O into the digestion vessel. The digestate was evaporated to near dryness and was re-dissolved in 10 ml of 5% HNO_3. Vials were sonicated for approximately 30 minutes and the solutions were transferred to 15 ml bottles.

Atmospheric and trap sediment (500-1000µm) samples were previously digested and reported for Fe and Al in Tian et al, (2008). Unpublished Mn and Zn atmospheric data (Tian et al., unpublished) along with reported values for Fe and Al were utilized for this study; however, trap digests were recovered and reanalyzed.

Suspended particle and sediment trap digests were analyzed using Inductively Coupled Plasma tandem Mass Spectrometry, (ICPMS-Agilent7500cx). For consistency, the ICPMS was calibrated with the same

multi-element standards (SCP Science) as used in the previous analysis of atmospheric and trap samples. The He-collision cell reduced potential isobaric interferences due to the matrix and argon carrier gas, and was run with analysis for all elements. Isotopes used for calculation included the following: Al-27, Fe-57, Mn-55 and Zn-66. Detection limits for the ICPMS were calculated for both sets of samples, by dividing three times the standard deviation of four blanks by the difference between the ion counts of a 1ppb standard sample and the average ion counts of four blanks (Table 2). Limit of detection values during trap analysis using the fusion method and ICPMS were previously reported (Table 3).

Table 2. Limits of detection for ICPMS during analysis for sediment traps and suspended particles compared to GFAAS.

LOD (nM)	Al	Fe	Mn	Zn
ICPMS	13.70	2.98	1.09	0.61
GFAAS	0.37	1.93	0.91	0.15

Table 3. Limits of detection for solid trap material (ng/g solution) determined from a fusion method, analyzed by HR-ICPMS (Huang and Conte, 2009).

LOD	Al	Fe	Mn	Zn
Trap Solids (ng/g solution)	7	0.2	9	0.07

Field blanks were not available for the trap samples or for the suspended particles during January or May, so the reagent blank of the 1% HNO_3 solution was used for blank correction. All samples were diluted 5x from

a 5% HNO_3 matrix to a 1% HNO_3 matrix for analysis using ICPMS. For trap samples, when the required dilution of the sample brought the ion counts beneath detection limit, the values previously determined by Tian and colleagues with Graphite Furnace Atomic Absorption Spectrometry (GFAAS) were used.

2.2.3 Additional Data

Several databases were utilized to further identify factors that may influence the distribution of the trace metals in the water column. Air mass trajectories were determined using the NOAA HYSPLIT Model (http://ready.arl.noaa.gov/HYSPLIT.php) for a period of ten days during three months in the sampling period (August, December and April). Models were used to identify the primary sources of atmospheric input to the sampling site. Conductivity, temperature, depth (CTD) data from the Bermuda Atlantic Time Series (BATS) database were used to better understand the physical properties of the water column during three sampling seasons. In particular, the temperature profile identified the mixed layer to later determine the depth of the reservoir for residence time calculations. Unpublished notes from the collection and splitting of the trap sediments were used, including the presence of salp fecal pellets and macrozooplankton. In addition, mass flux and organic carbon in traps, determined by collaborators (Conte Lab), were used for further data synthesis.

2.3 Results and Discussion

2.3.1 Seasonal Air Trajectories and Atmospheric Input

Backward trajectories using the NOAA HYSLIPT Model during August ’99, December ’99 and April ’00 illustrate differences in the air masses arrived in Bermuda between seasons (Figure 2). This model can be a useful tool to track dust events that may impact solubility (Sedwick et al., 2007). However, the purpose of using the model in this investigation was to highlight the origin of atmospheric deposition and potential influencing sources. The 10-day air trajectory for August represents the air masses delivering aerosols to Bermuda during the summer (Figure 2a). Saharan dusts were traveling southwest and are carried over the southeastern part of the U.S. in a clockwise direction before reaching Bermuda. It is therefore expected that the aerosol had a primarily crustal composition of the aerosols with anthropogenic influences. In December, atmospheric deposition appears to be entirely from the northern U.S. (Figure 2b), thus, an even mixture between crustal and anthropogenic aerosols during this time. During April, yet another source of aerosols are displayed (Figure 2c). The source of aerosols was more northern in origin, from the region of the Labrador Sea.

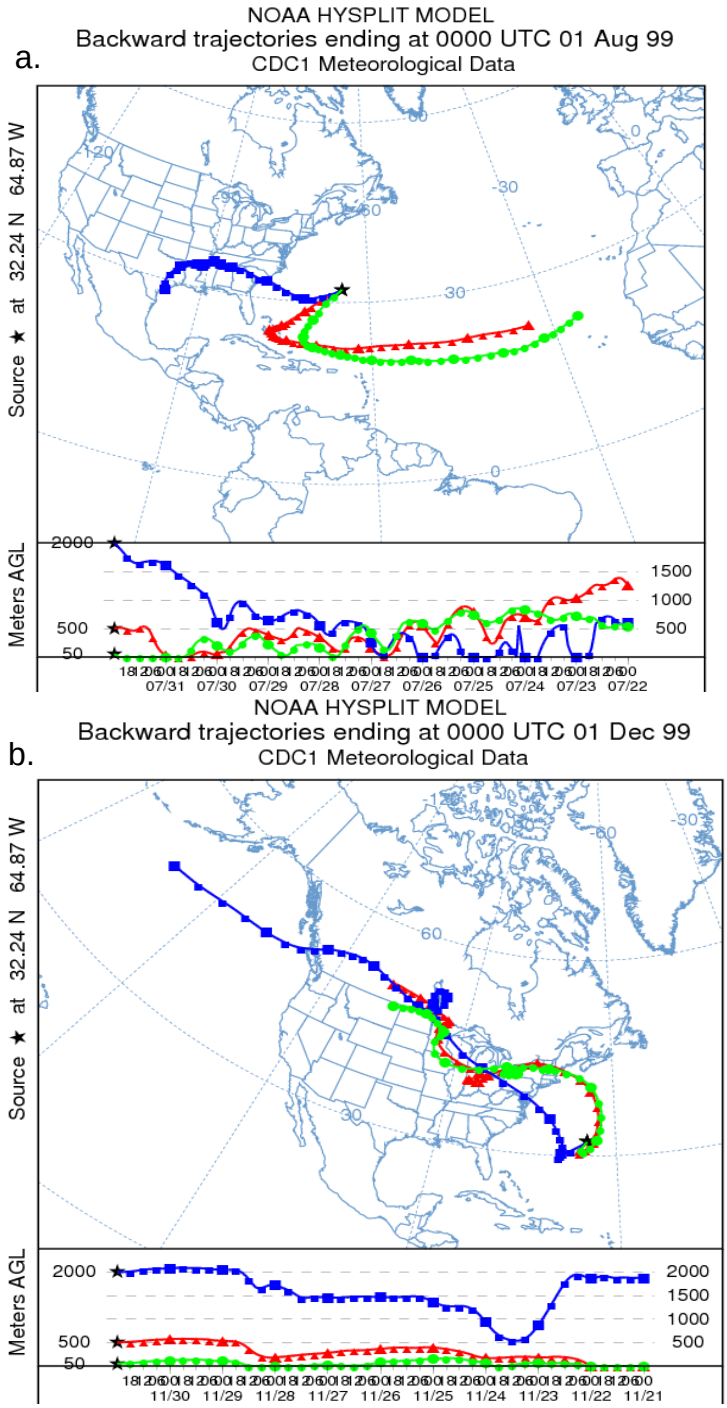

Figure 2. Air mass back trajectories for a) August '99 b) December '99 and c) April '00, from NOAA HYSPLIT Model.

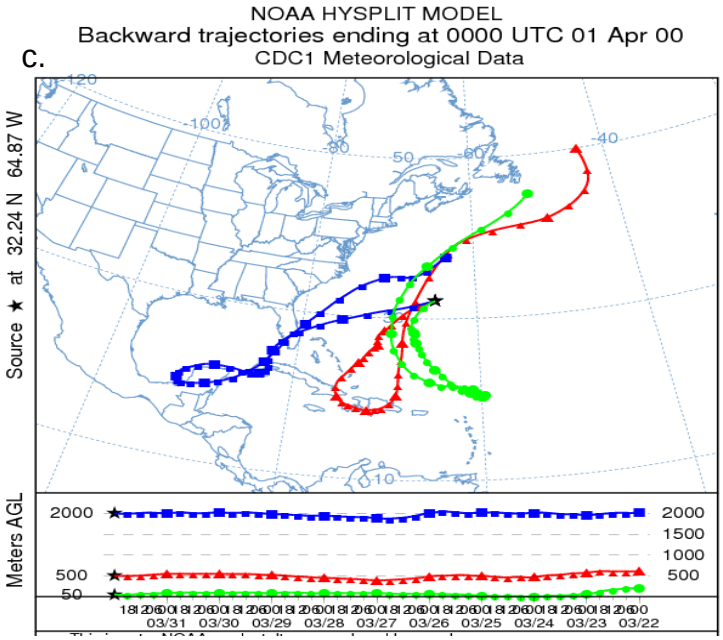

Figure 2. Continued.

Average values for both wet and calculated dry (bulk – wet) deposition for the entire period are shown in Figure 3. Throughout the sampling period (July 1999 to April 2000), calculated dry deposition of Fe, Mn and Zn dominated the bulk atmospheric flux by more than 80%. Dry flux has not always dominated the total input in other years reported at Bermuda. For example during sampling years previous to 1999 wet deposition of Fe represented more than 50% of the total atmospheric flux (Kim et al., 1999). Even with variability in the depositional modes, lithogenic elements in dry input have been shown to be less soluble than in wet deposition. The solubility is influenced by factor such as the surrounding pH, making the elements more labile (Church et al., 1984). Results indicate that it is the presence of organic ligands in rain, increase the solubility and in turn bioavailability of the elements (Kieber et al., 2005). In a

recent study, ^{7}Be and rainfall collected at the Bermuda tower over a two-year period was compared to that of the flux delivered to the Sargasso Sea. Results suggest that the bulk sampler may underrepresent ^{7}Be and rainfall that is delivered to the Sargasso Sea by roughly 40% (Kadko and Prospero, 2011). This suggests the underestimated influence on the delivery of trace elements to the open ocean by wet deposition.

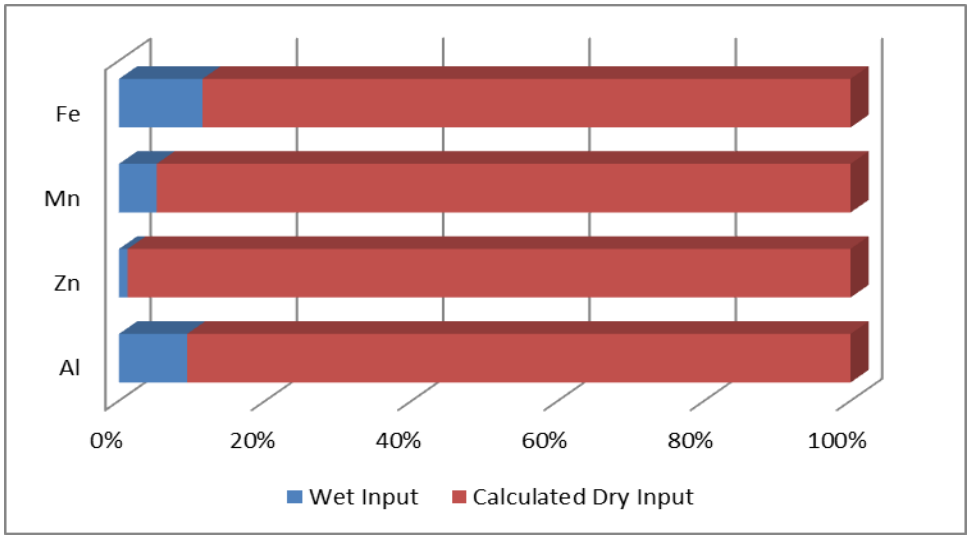

Figure 3. Average molar percentage of wet to calculated dry (bulk – wet) input for the entire sampling period (July 1999- April 2000).

Molar flux ratios of Fe, Mn, and Zn to Al in wet deposition were used to calculate enrichment factors and determine the origin of the metal, as crustal or non-crustal (Table 4). This calculation was based on the assumption that all Al in the atmospheric data as well as in the sediment traps was lithogenic. Throughout the sampling period, wet deposition was enriched with

Fe for all months except January (12/20-1/20/00). Maximum enrichment for Fe occurred during December (11/24-12/20/99). Conversely, molar ratios for Mn and Zn were closer to crustal values during December in comparison to the rest of the data set.

Calculations were performed in the same manner using values for dry deposition determined from the difference between collected bulk and wet deposition (Table 5). As with wet deposition for Fe, enrichment factors for December differed from typical crustal values. However, instead of maximum enrichment for Fe during December, a deficiency in Fe was observed. In addition, the maximum enrichment occurred in the following month. Data for Mn and Zn suggest additional input, other than crustal. In addition, periods of high enrichment for Mn appear to correspond with periods of high enrichment in Zn. Although it is difficult to contaminate samples for Mn, if the enrichment value for 3/14-4/14/00 is removed from the set, enrichment for the entire period Mn and Zn data correlate R^2=0.76 (Fig. 4).

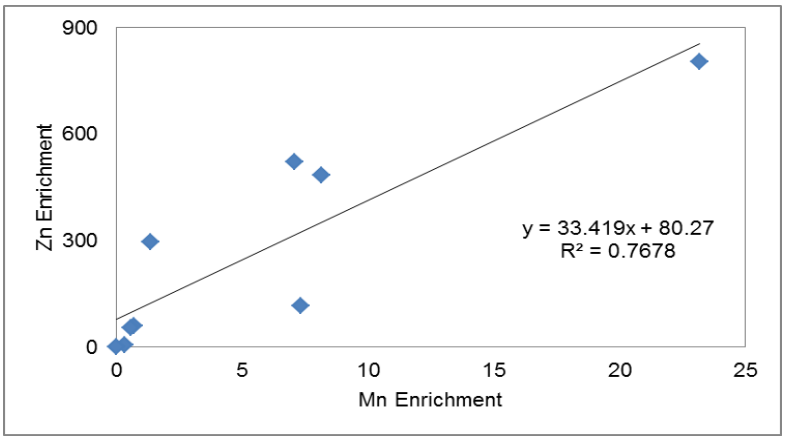

Figure 4. Relationship between Mn and Zn enrichment in the calculated dry flux from Jul '99 to Apr '00 (excluding data point for 3/14-4/14/00) in relation to crustal ratios.

Table 4. Atmospheric molar flux ratios of Fe, Mn, and Zn to Al in wet deposition collected monthly from July through mid-April. The average for the entire sampling period was considered, in relation to crustal ratios to predict crustal or non-crustal origin (Taylor and McLennan, 1985).

Sampling period	Fe/Al	Fe (Enrich.)	Mn/Al	Mn (Enrich.)	Zn/Al	Zn (Enrich.)
7/5-8/2/99	0.21	1.03	0.009	2.34	0.003	19.0
8/2-9/7/99	0.27	1.31	0.012	3.20	0.012	76.2
9/7-9/28/99	0.25	1.21	0.013	3.44	0.011	72.5
9/28-10/25/99	0.30	1.46	0.015	4.01	0.005	31.5
10/25-11/24/99	0.31	1.51	0.017	4.66	0.034	221.0
11/24-12/20/99	0.47	2.27	0.004	1.20	0.002	11.6
12/20-1/20/00	0.08	0.41	0.003	0.82	0.013	85.3
1/20-2/18/00	0.24	1.18	0.016	4.36	0.040	262.0
2/18-3/14/00	0.40	1.93	0.025	6.94	0.043	278.0
3/14-4/14/00	0.26	1.26	0.015	4.18	0.008	49.9
Average	0.28	1.36	0.013	3.51	0.017	111.0
Molar Crustal Ratio	*0.206*		0.00366		0.000153	

Table 5. Atmospheric flux (nmol m^{-2} d^{-1}) ratios of Fe, Mn, and Zn to Al in calculated dry deposition (bulk – wet) collected monthly from July through mid-April. The average for the entire sampling period was considered, in relation to crustal ratios to predict crustal or non-crustal origin (Taylor and McLennan, 1985).

Sampling period	Fe/Al	Fe (Enrich.)	Mn/Al	Mn (Enrich.)	Zn/Al	Zn (Enrich.)
7/5-8/2/99	0.26	1.27	0.002	0.60	0.003	17.7
8/2-9/7/99	0.21	1.03	0.005	1.37	0.023	148.0
9/7-9/28/99	0.30	1.47	0.010	2.76	0.110	722.0
9/28-10/25/99	0.29	1.41	0.061	16.60	0.181	1180.0
10/25-11/24/99	0.19	0.90	0.055	14.90	0.044	287.0
11/24-12/20/99	0.04	0.21	0.004	1.16	0.020	131.0
12/20-1/20/00	0.33	1.58	0.053	14.40	0.195	1270.0
1/20-2/18/00	0.25	1.22	-	-	-	-
2/18-3/14/00	0.24	1.19	0.173	47.20	0.300	1960.0
3/14-4/14/00	0.19	0.93	6.919	1890.00	0.282	1840.0
Average	0.23	1.12	0.728	199.00	0.116	756.0
Molar Crustal Ratio	*0.206*		0.00366		0.000153	

Anthropogenic influence impacts Zn and Mn as well as Fe to a lesser degree. Kim et al. (1999), reported that more than 90% of Zn deposited in Bermuda originates from non-crustal sources, determined from enrichment calculations. Although Mn behaves similarly to lithogenic Fe and Al, it also shows a high percentage of non-crustal sources and can be greater than 50% of total Mn input to Bermuda. With emissions from anthropogenic input, it is likely that these aerosols are efficiently scavenged by rain. Increased solubility of metals from emissions have been speculated to be due to the acidic inorganic and organic species that are present in the atmosphere and mediate reductive dissolution (Sedwick et al., 2007). For enrichment factors with

values above crustal in our own data, we would expect to see this anthropogenic input and increase in solubility.

It is possible, and suspected in several of our samples that there was some contamination introduced to the bulk samples. A few anomalies occurred in the bulk data that led us to utilize the values for wet deposition and assume a lower atmospheric estimate of the flux. Fe and Al correlated positively for the entire period (R^2=0.81), indicating that the source was largely lithogenic. However, one point in the sampling period (11/24-12/20/99) deviated from the best fit, indicating higher Al enrichment. Suspecting contamination of the sample, we have found that removal of this point results in a higher degree of linearity (R^2= 0.99), as shown in Figure 5. It appears that the supply of Fe and Al to the surface ocean during the entire sampling period was most likely lithogenic in origin.

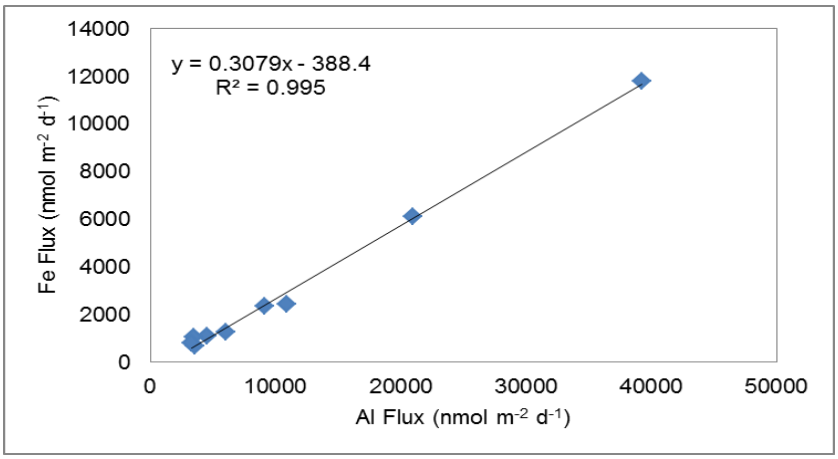

Figure 5. Relationship between Al and Fe in the bulk atmospheric flux from Jul '99 to Apr '00. This data excludes the data point for December, in which an additional source of Al was suspected.

It is more difficult to identify contamination in Mn and Zn data in the same manner, as both elements have anthropogenic sources. However, in this study where there are several high flux values, we suspect that this was most likely cause by bird droppings captured in the bucket for bulk collections during periods of bird migration. Taking note of high bulk flux values for several points, we chose to mainly focus on the wet data. We acknowledge, however, the large contribution of these elements to the Sargasso Sea by both wet and dry deposition. Wet deposition may be the lower estimate of total input to the surface ocean, but it also contains elements in a speciation that is more likely to be bioavailable to organisms.

2.3.2 Comparing Atmospheric Input and Traps

For Fe, both the wet atmospheric flux and trap fluxes varied seasonally from July 1999 to April 2000 for Fe (Fig. 6). There was a maximum

of atmospheric input during December (Fig. 6a), which also appeared in the 500 m trap (Fig. 6b). However, the output flux at the 500 m trap was greater by nearly 25- fold than wet deposition. There was a maximum of Fe flux during the late fall for both the 1500 m and the 3200 m traps (Fig. 6c, 6d). Although there was a moderately strong positive correlation between the mid and deep water traps during the sampling period (R^2= 0.78), there was none with atmospheric deposition. However, there were periods of positive correlation between atmospheric input and trap flux. From July to October there was a strong positive correlation of R^2= 0.996, and there was a moderately strong positive correlation further in the period to December R^2=0.73. From January to April the same correlation exists R^2=0.73, however for the entire set there is no significant correlation.

Mn fluxes were compared with Fe for both atmospheric deposition and flux collected at the mid and deep traps (Fig. 7). Excluding December, the atmospheric flux of Mn and Fe are strongly correlated positively (R^2= 0.91) (Fig. 7a). Although the increase in the atmospheric flux of Mn during December was not present, the sharp increase in flux occurred in the 500 m trap (Fig. 7b). Like Fe, the mid-water and deep-water traps also agreed (R^2= 0.59) for the entire sampling period (Fig. 7c, 7d). However, the Mn fluxes were much smaller relative to Fe. Mn flux at the 1500 m and 3200 m traps were roughly 10-fold less than the Fe Flux. There was a positive correlation between the wet atmospheric deposition and the trap flux occurred during the last three months of the sampling period, R^2= 0.58

The atmospheric input of Zn as well as distribution in deeper traps differed from that for Fe and Mn (Fig. 8). Although the sharp increase in atmospheric flux for Zn is not observed in December (Fig. 8a), it is present in all trap depths (Fig. 8b, c &d). Unlike Fe and Mn, there was not a significant correlation of Zn fluxes between the 1500 m and 3200 m traps. However, the flux increased in the 500 m traps highlight three periods of increased input: August, December and April. This result is observed for Fe and Mn at 500 m, however is not as apparent due to the input in the bordering months.

In the mid and deep-water traps, we found similar relationships between Al (Fig. 9), Fe and Mn at both depths. The strongest positive correlations were between Al and Fe at 1500 m (R^2= 0.97) and at 3200 m (R^2= 0.95). Mn was positively correlated with both elements at 1500 m (R^2=0.87), however did not correlate significantly with either elements in the 3200 m trap. This was unexpected due to the results of Mn enrichment calculations, in which the traps at 1500 m were more enriched in Mn than traps at 3200 m.

There was a high period of wet deposition for Fe, Mn and Zn that occurs from July to October, and was at a maximum during August. One cause for this is the scavenging and washout of fine particles from Saharan dusts containing Fe, Mn and Al along with Zn and Mn in aerosols from combustion emissions. Influence from North America (including emissions) can be implied from the back trajectory observed from the NOAA HYSPLIT Model (Fig. 2a).

The increase in atmospheric flux of Fe in December in relation to other elements is supported by findings in Wolff et al. (1987), in which washout ratios were calculated from trace metals including Fe, Mn, and Zn during summer and winter. When of crustal origin, Fe associated with fine particles were found to be strongly associated with Mn associated with fine particles. There was a correlation between Fe and Mn during summer (R^2= 0.98), when the source of particles was from Saharan dusts, whereas there was a positive correlation during winter (R^2= 0.78). The study attributed the enrichment in Fe to additional sources in the winter.

In this investigation, if the additional atmospheric input were anthropogenic in origin, from emissions, the Fe could in turn be scavenged into wet deposition and may be more bioavailable to organisms. Winter atmospheric events are typically dominated by air trajectories from North America, as observed in the back trajectory from the NOAA HYSPLIT Model for December (Fig. 2b). In comparison to air trajectories from the Saharan, North American air contains relatively lower loading of Fe, congruent with a higher fractional solubility (Sedwick et al., 2007). This trend most likely extends to Mn and Zn, as aerosols from North America are typically a mix of crustal and anthropogenic sources, such as from fuel-combustion.

Total trap fluxes for all elements from July to April were variable relative to each other at all depths (Fig. 10). However, trends for Fe and Al were most closely related (Fig. 10a, d). Although the total wet atmospheric input was less than total trap flux at all depths, in all cases, the bulk flux (wet + dry was larger than the 500 m flux for some elements. These elements include Mn, Zn and to

a lesser degree Al. From the 500 m trap, there was a large increase in Fe, Mn and Al fluxes to the 1500 m traps, whereas there was a decrease in Zn flux from the 500 m to 1500 m trap.

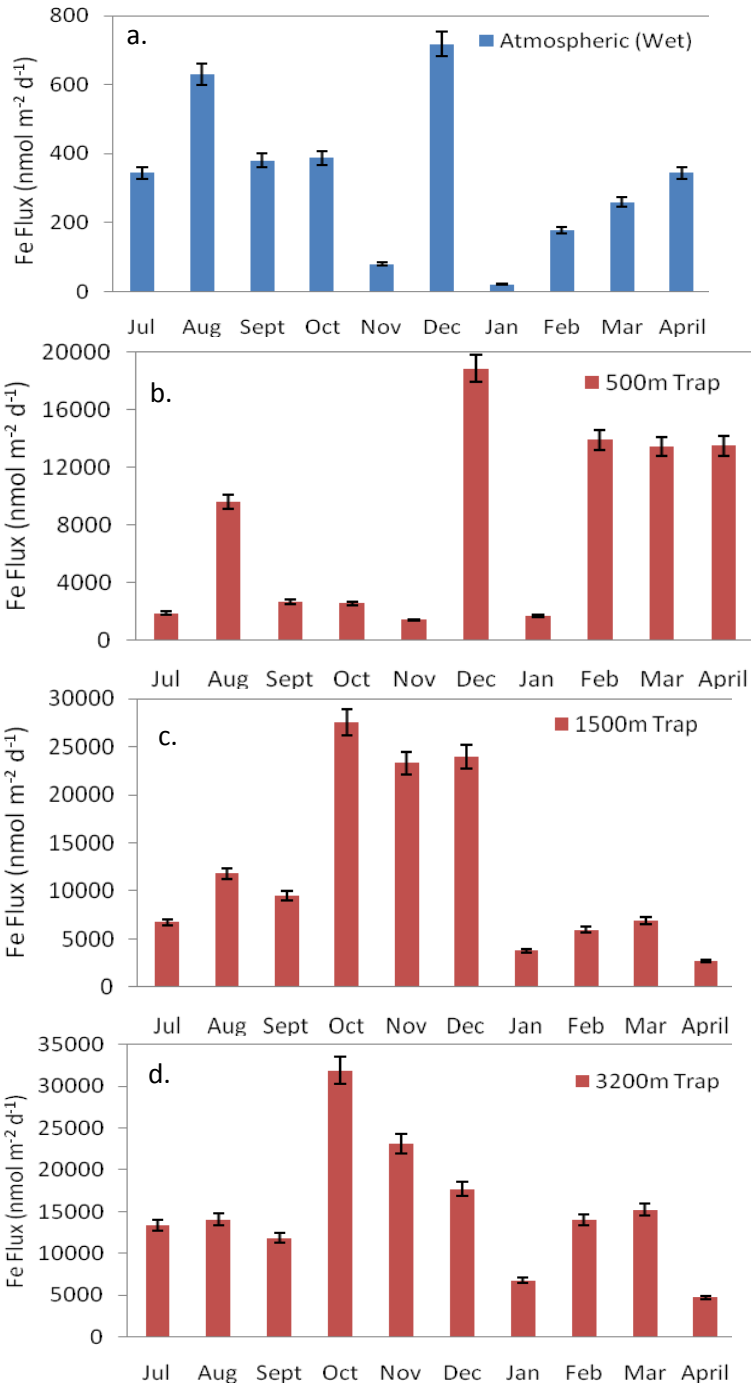

Figure 6. Total monthly flux of Fe in wet atmospheric input and in sediment traps.

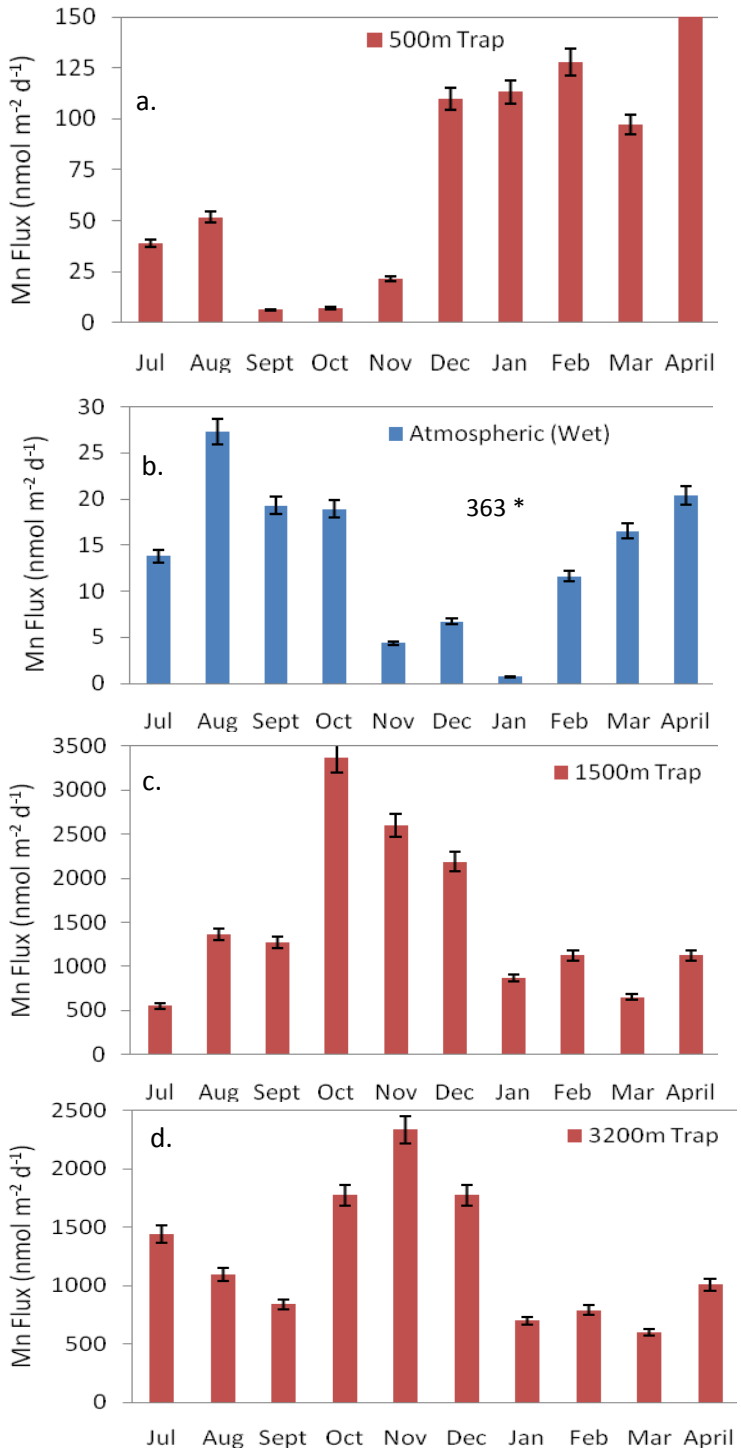

Figure 7. Total monthly flux of Mn in wet atmospheric input and in sediment traps.

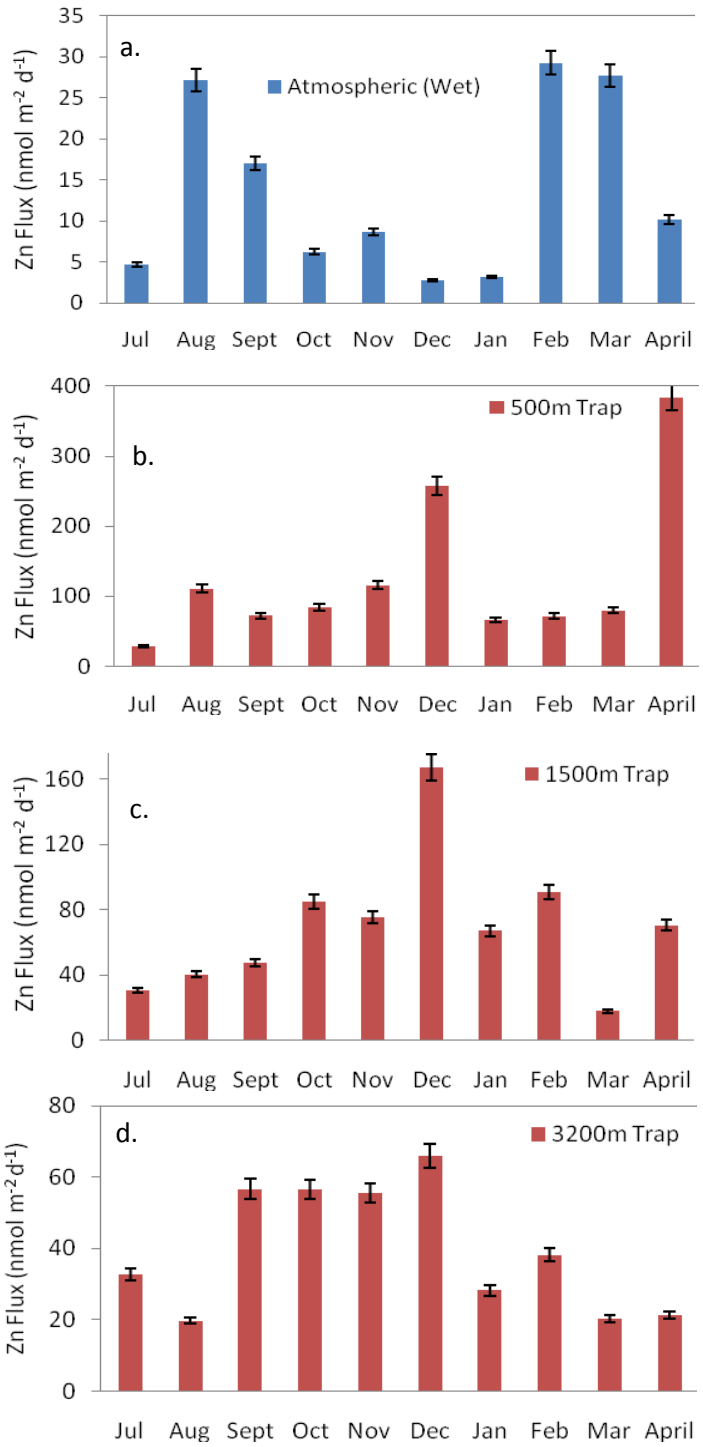

Figure 8. Total monthly flux of Zn in wet atmospheric input and in sediment traps.

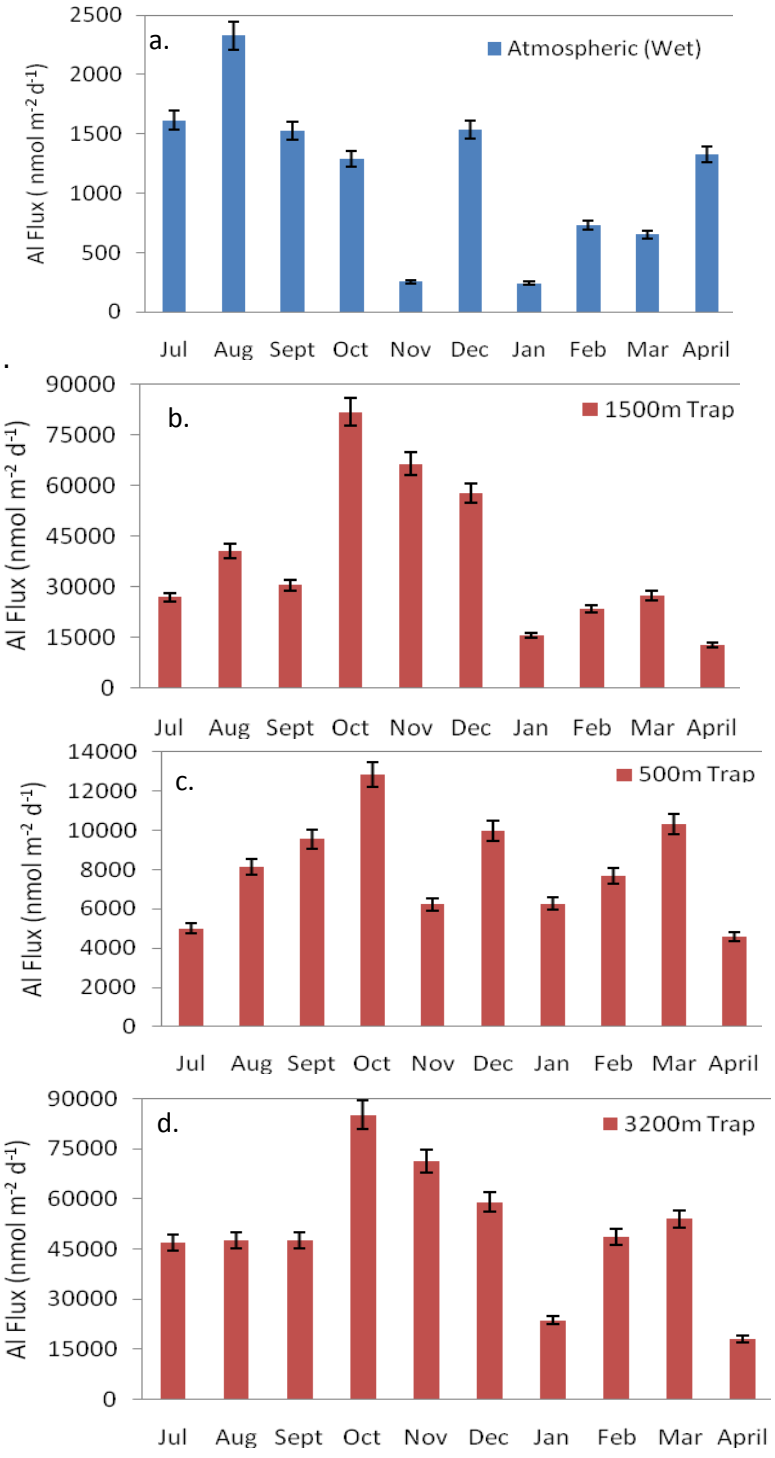

Figure 9. Total monthly flux of Al in wet atmospheric input and in sediment traps.

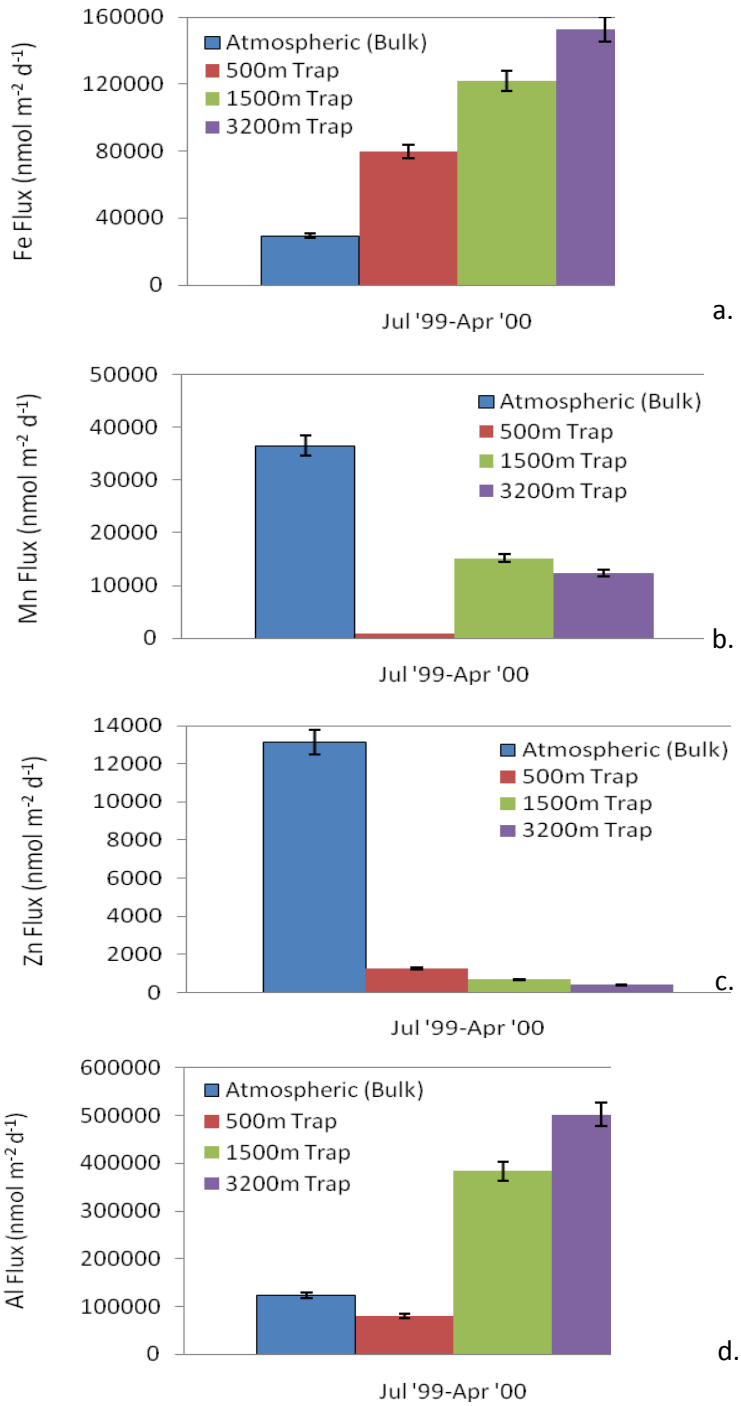

Figure 10. Total flux of Fe, Mn, Zn and Al for bulk atmospheric input and sediment traps.

Jickells et al. (1984) reported that the flux calculated for wet deposition in the BATS region was enriched in Zn relative to that in sediment traps. In addition, it was speculated that there are additional sources of Fe and Mn to deep waters. The 500 m flux for Mn and Zn could be accounted for by the bulk atmospheric flux in this study. Instead the discrepancy was observed in the deeper traps for Al and Fe. There were higher Al and Fe fluxes in deep traps in relation to bulk atmospheric input, indicating additional sources. On the other hand, the trap fluxes in both Mn and Zn flux in the mid and deep water were comparable to the bulk input.

At times during the sampling period there was a coupling between the wet atmospheric input and the 500 m trap. During the first three months of the sampling period, including August, there was a strong positive correlation for input of Fe and Zn with the trap flux during that period ($>R^2= 0.99$). During the late winter to early spring (January through March) all elements in wet input were moderately strong to strongly correlated positively with traps (Fe: $R^2=0.64$, Mn: $R^2=0.58$, Zn: $R^2=0.998$, Al: $R^2=0.87$). During the winter, however, Fe was the only element that was coupled between wet atmospheric input and the surface trap. This suggests comparable adsorbing and mixing for all elements during December, as indicated by the increase for these elements in flux in the 500 m.

The biological influence on the distribution of trace metals observed in the upper water column during winter can be explained by the sinking of smaller blooms due to increased convection caused by brief winter storms (Ueyama and Monger, 2005). Although particle aggregation is a

contributing factor to the downward flux, it is thought that aggregation is only prevalent during production periods of high-biomass (Lomas et al., 2009), like during the spring bloom. The pulse of mass flux during the winter was also reported in Conte et al. (2003), and was considered typical between December and March. Although only the deep water trap was sampled in the reported study, results suggested that this flux should have been observed in the shallow trap as well.

2.3.3 Mass Flux and Notes on Sediment Traps

Complementary data to the sediment trap analysis include work done by Maureen Conte's lab at the Marine Biological Laboratory. Parameters such as the mass flux and a record of what was observed in the trap cup upon collection were used to further interpret the distribution of Fe, Mn and Zn in the trap sediments. The transport of large particles influences the distribution of trace elements in the dissolved and suspended particle flux, which signifies the importance of these data.

Total mass fluxes for each sampled month displayed seasonal variation over the entire period (Fig. 11). Highest mass fluxes are observed in the summer to early fall season as well as in the late winter into spring. In particular comparable sediment mass fluxes were delivered to traps at all three depths during February and March. This period is significant as it coincides with the spring bloom, in which zooplankton would be grazing and rapidly repackaging organic material into large, downward fluxing particles. Although the late summer to early fall period does not typically support phytoplankton growth and bloom, it is a time when dust events are more

frequent (Tian et al., 2008). In addition, there are zooplankton that rapidly process lithogenic materials into downward fluxing particles.

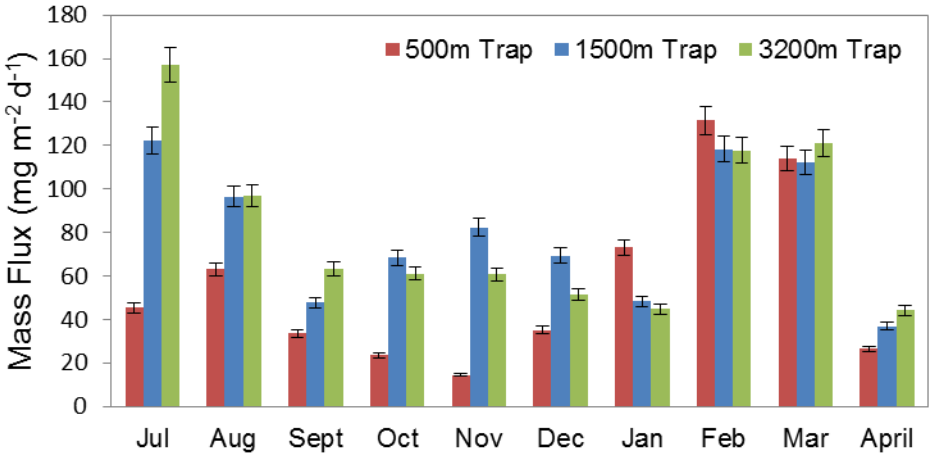

Figure 11. Total mass flux for each sampled month at three trap depths.

Reported observations upon the recovery of the sediment trap samples are shown in Table 6. High frequencies of salp fecal pellets were observed upon the recovery of sediment traps collected from the end of summer through the fall. Salps are significant primarily because they rapidly produce large, organic-rich fecal pellets that can sink at rates ranging from 43-2700 m d^{-1} (Turner, 2002). The largest amount of salp pellets were recorded to have been present in the 1500 m and 3200 m trap, with trap dates coinciding with pellets that were also recovered in the 500 m traps. A possible explanation for this is the diel vertical migration of salps (Turner, 2002), thereby influencing the distributing of the downward sinking flux. In addition, the catchment area may play a role in the larger flux observed in the deeper

traps. Salps are not selective feeders, which suggest that fecal pellets would reflect total input. If input were not soluble and crustal, this composition would be reflected in the sediments collected in the trap.

Swimmers' were observed in the 500m trap during two different seasons, however were most prevalent during the winter. Swimmers refer to large zooplankton that are caught in the trap cup, as they are grazing. In particular, swimmers such as fish are significant, because they contain high levels of Fe due to the hemoglobin contained in blood. Therefore they pose a potential source of contamination. During December, when a high flux of Fe is observed in the 500m trap there were also fish found in the trap cup. Although there is an increase in atmospheric Fe delivered to the open ocean during that time, the swimmers may have attributed additional Fe to the sample, as was observed.

Table 6. Observations recorded during trap sample recoveries, including the presence of salp fecal pellets, swimmers, and anoxic conditions (Conte et al., unpublished). Bolded items indicate large abundance.

Month	Trap ID	500m	1500m	3200m
July- 1999	9/99-3	SFP	SFP	SFP
	9/99-4	SFP	**SFP**	**SFP**
August- 1999	9/99-5	F	SFP	SFP
	9/99-6	SFP	SFP	SFP
	9/99-7	-	SFP	SFP
September- 1999	9/99-8	F	-	SFP
	1/00-1	S	-	-
October- 1999	1/00-2	S	-	-
	1/00-3	-	-	-
November- 1999	1/00-4	-	-	-
	1/00-5	F	-	-
December- 1999	1/00-6	F	-	-
	1/00-7	-	-	-
January- 2000	5/00-1	-	-	-
	5/00-2	-	-	-
February- 2000	5/00-3	A	R	-
	5/00-4	A	R	-
March- 2000	5/00-5	A	R	-
	5/00-6	A	R	-
April- 2000	5/00-7	A	R	-
	5/00-8	-	R	-
	5/00-9	-	R	-

SFP= Salp fecal pellets F= Fish
S= Shrimp R= Radiolarians
A= Anoxic conditions - = no swimmers or salp fecal pellets found in trap cup

2.3.4 Suspended Particles

Element distributions in depth profiles for suspended particles varied between the two sampling seasons, but were comparable between

some elements (Fig. 12). Maximum concentrations for Fe, Al, and Zn profiles occurred at ≤ 500 m, however, the maximum for May occurred < 1000 m. For Fe, a sharp maximum occurred in particle concentrations in the upper 100 m up to nearly 2 nM in January and 1.5 nM in May (Fig. 12a). With depth, the concentration decreased in the January profile and increased in the May profile before intersecting at ~1.0nM at 1500m. In comparison with the Al profile (Fig. 12b), although there is variability in the upper 100 m of the January profile for Al, the overall trend is comparable (R^2= 0.60). However May profiles for Al and Fe agree strongly (R^2=0.994). The maxima for Mn occurred at different depths between each season (Fig. 12c). The seasonal profiles for Zn and Mn have comparable relationships in the surface and deep waters (Fig. 12c, d). In depth above 500m, Zn has a negative correlation with Mn (R^2= 0.61 in January and R^2=0.95 May). However, after 500 m Zn positively correlates with Mn with comparably agreement.

Similar relationships were observed in previously reported particle profiles from the same sampling site, in which Al- Fe and Mn-Zn were categorized together (Sherrell and Boyle, 1992). Literature profiles were collected during March, 1988 using 0.53 µm filters (Nucleopore), and were added to profiles from this study for comparison (Fig. 12). Although concentrations were in the same order of magnitude, the reported investigation observed larger concentrations in the mid to deep water samples. On the other hand, larger surface enrichment of some element profiles was observed in this study that was not observed in the reported profiles. This may be due to natural variation in the sampling year or that the

surface particles in the upper 100m were collected during March, April and September and may not reflect the surface in this study.

Consistency between profiles for Al and Fe was observed with depths below 1000m. In this investigation, profiles correspond at the surface as well, even between seasons. The overall shape of the reported profiles for Al and Fe resemble to profile for May in this study, with surface enrichment, depletion, relatively uniform concentrations to nearly 3000m and increased concentration in the deep water. Parallel profiles indicate that both Al and Fe in particles are predominantly in the same phase. Sherrell and Boyle (1992) reported that particulate profiles for Mn and Zn were similar in that there was a decrease to relatively uniform concentrations beginning around the mid-thermocline. We observed this feature in the profiles for both elements around 500 m.

Elemental ratios to Al were also compared between this study and calculations made from particle data reported in Sherrell and Boyle (1992) that were collected in March, 1988 (Tables 7 and 8). We observe closest agreement to crustal ratios in the surface- most samples during the May collection. However, Fe and Zn display values closer to crustal in the deepest sample for both months as well. The Fe profile deviates from crustal and shows enrichment in the surface particles in the January samples. Ratios calculated for the literature data were consistently closer to crustal values throughout the profile, however the average for Fe and Zn compare with the May profile in this investigation. Values that differ from crustal can be

explained by the collection of biogenic particles and phytoplankton on the particle filter.

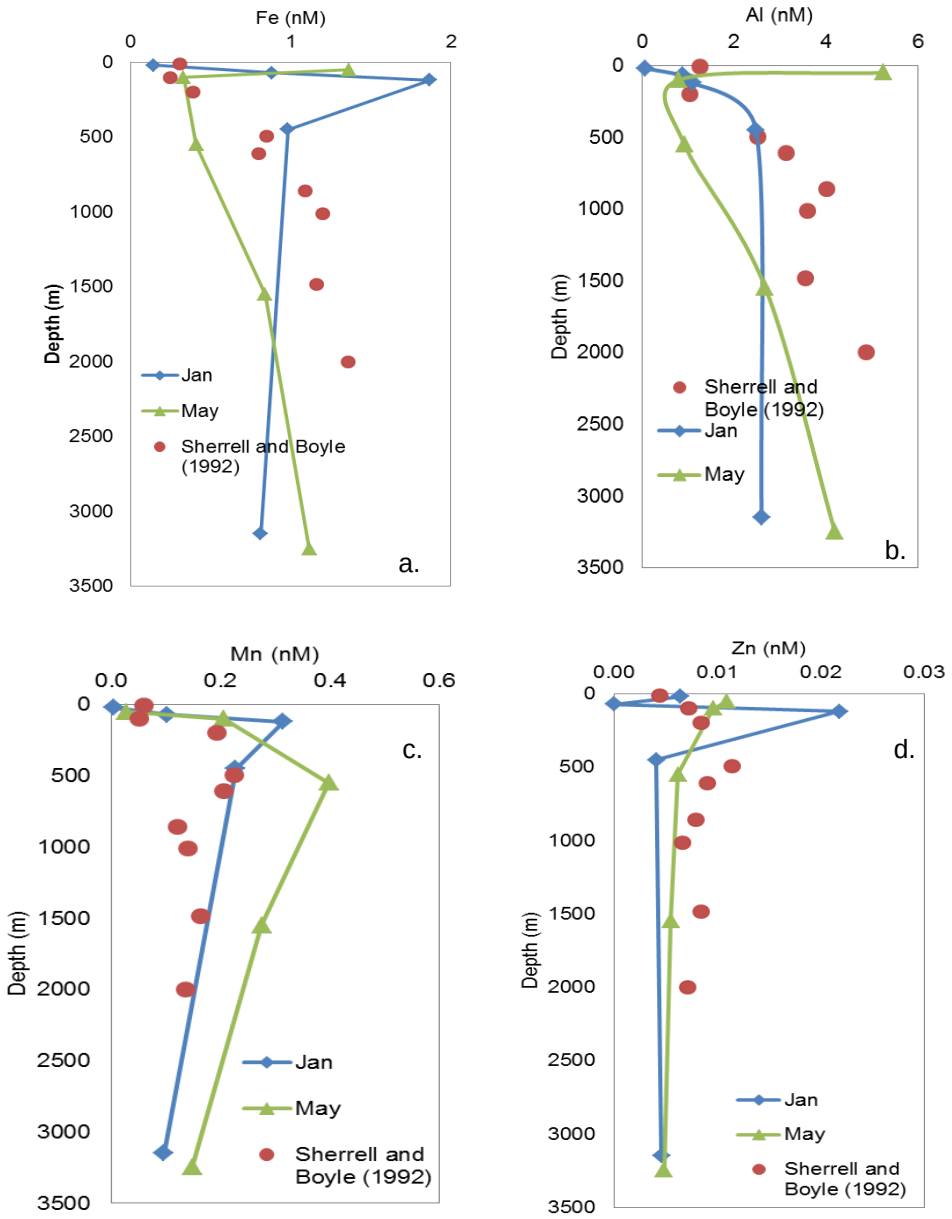

Figure 12. Suspended particle profiles for a) Fe b) Al c) Mn and d) Zn from January and May 2000 compared with literature profiles from March, 1988 reported in Sherrell and Boyle (1992).

Table 7. Calculated elemental ratios (nmol/nmol) for particle profiles with monthly averages determined for January and May. *Literature crustal ratios (Taylor and McLennan, 1985).

Month, Year, Depth (m)	Elemental Ratio (nmol/nmol)		
	Fe/Al	Mn/Al	Zn/Al
Jan00-20 m	1.78	0.0664	0.07938
Jan00-70 m	0.99	0.1156	-
Jan00-120 m	1.70	0.2857	0.01980
Jan00-450 m	0.40	0.0920	0.00167
Jan00-3150 m	0.31	0.0369	0.00178
Avg.	1.03	0.1193	0.02566
May00-50 m	0.26	0.0053	0.00209
May00-100 m	0.41	0.2582	0.01205
May00-550 m	0.44	0.4330	0.00674
May00-1550 m	0.31	0.1028	0.00205
May00-3250 m	0.27	0.0354	0.00116
Avg.	0.34	0.1669	0.00482
*	0.206	0.00366	0.000153

Table 8. Calculated elemental ratios from suspended particle data reported for cruise WE 388, 3/12-13/88 at 32˚12N, 64˚28W (Sherrell and Boyle, 1992). *Literature crustal ratios (Taylor and McLennan, 1985).

Depth (m)	Elemental Ratio nmol/nmol)		
	Fe/Al	Mn/Al	Zn/Al
10	0.25	0.047	0.004
100	0.27	0.055	0.008
200	0.38	0.188	0.008
494	0.34	0.089	0.005
608	0.25	0.066	0.003
861	0.27	0.030	0.002
1013	0.33	0.039	0.002
1483	0.33	0.046	0.002
2000	0.28	0.028	0.001
Avg.	0.30	0.065	0.004
*	0.206	0.00366	0.000153

2.3.5 Upper Ocean Residence Times

Residence time calculations were modified using a simple box model, as described in Croot et al. (2004). We followed the general equation: $\tau = M/J$, where M is the reservoir size and J is the flux (input or output) multiplied by the solubility of the element. Separate calculations were performed for the input flux (soluble wet + soluble calculated dry) and for the output flux (500 m trap). The reservoir size was calculated by volume weighted averages from depth profiles of the dissolved fraction. Depth intervals for the reservoir size were estimated for three seasons using temperature profiles from CTD casts, in which the mixed layer was identified (Fig. 13).

The soluble fraction of the dry deposition was determined by modified calculations from (Sarthou et al., 2003), $F_{dry} = C_{AM}\, v_d$, in which C_{AM} is the estimated average concentration of the metal deposited over one year. This term excludes different calculations for coarse and fine mode deposition. The term v_d is the deposition velocity, in which 1 cm s^{-1} was used due to the presence of both fine and coarse particles during the sampling period. If fine and coarse mode can be distinguished, we would use 0.1 cm s^{-1} and 2 cm s^{-1} as the deposition velocities. The solubility values used for each element in dry deposition were as follows: Fe-10% (Sedwick et al., 2005), Mn-60% (Sholkovitz et al., unpublished data) and Zn-30% (Chester et al., 1993). Wet flux (F_{wet}) was calculated as the average flux of the metal for the sampling period estimated for one year. The data available for wet deposition was only available in units of flux, with the precipitation rate for the year already integrated into the data. The solubility values used for each element in wet

deposition were as follows: Fe-14%, Mn-64% (Jickells, 1995) and Zn-96% (Lim et al., 1994).

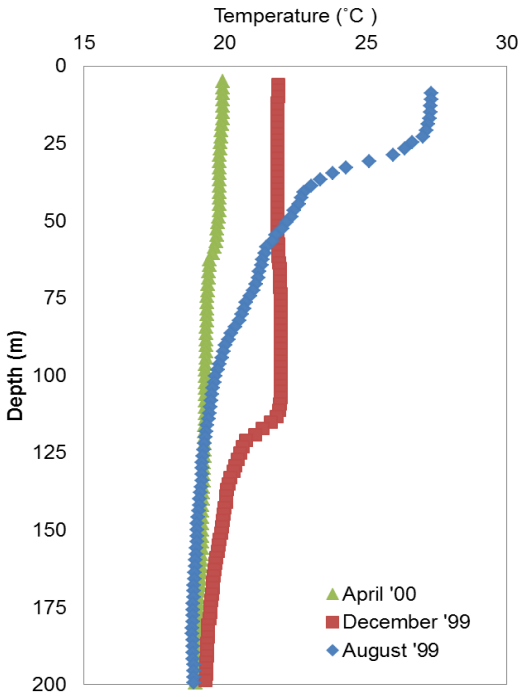

Figure 13. Temperature profiles from CTD data collected by BATS, during seasonal cruises.

Calculations compared input atmospheric flux ‘source’ of trace metals to the downward ‘sink’ into the 500 m trap, in which a difference in residence times between calculations were observed (Table 9). Seawater profiles reported in (Milne et al., 2010) were used to determine the dissolved reservoir for Fe, Mn and Zn at three depth intervals determined by the mixed depth of all three elements, Mn represented the largest reservoir during all

seasons (85 nmol/m^2 during Jul-Sept, 203 nmol/m^2 during Oct-Dec and 270 nmol/m^2 during Jan-Apr). The dissolved reservoir was combined with the suspended particle reservoir, from the May suspended particle samples, to obtain a 'total' reservoir.

We acknowledge the influence of lateral advection, but we have not included this variable term into our calculations. However, we have estimated the contribution by taking the difference between the input flux (wet + calculated dry) and output flux (Table 9). We found a net lateral flux of Mn and Zn into the box at each depth range and season. Conversely there was a net output flux of Fe out of the box during each depth range except for the surface 50 m, during Jul-Sept. Results suggest that lateral advection of surface dusts are seasonal, possibly due to the increased mixing typical during the winter and spring.

Residence times varied between calculations with the input and output values as well as between seasonal reservoirs. Calculations using input resulted in the largest range of residence times for Fe, Mn and Zn. The range for Fe when using input flux was nearly 20-fold, whereas the range of residence times for Fe were only three-fold range when using the output flux. For Mn, a 60-fold range was determined when using input flux but only a six-fold range when using output flux. For Zn, the range was 18-fold for calculations with input flux and two-fold when using the output flux. The residence times for Fe, Mn and Zn were also calculated over the entire period, considering the reservoir from the surface to the 500 m trap (Fig. 14). The

calculated residence time for Fe was nearly three-fold greater than Mn, and the residence time for Mn was nearly two-fold greater than Zn.

Residence times for Fe and Mn in the surface 100 m for total deposition and dissolved deposition were previously reported (Jickels, 1999). The reported residence time for total Fe was 17.9-18.1 d. Mn had a longer reported residence time, ~1800-1900 d in the upper 100 m. Relatively short residence times ranging from 6-62 days in the upper 200 m were calculated for total Fe (Croot et al., 2004). Furthermore, the reported investigation indicated that repeating the calculations using the mixed layer (50 m) would result in a decrease in residence time by 4-10 times. In another study, Fe was reported to have a residence time of 1-5 months in the surface waters of the N. Atlantic (Berquist et al., 2007). Values calculated for Fe were closer to literature values in surface waters. On the other hand, the residence times for Mn calculated using the output flux were closer to literature values than with the input flux but were still low.

Table 9. Seasonal residence times for total Fe, Mn and Zn (dissolved + May suspended particles) at three depth intervals. The trap flux output and wet and dry input were averaged over three months during each season from July 1999 to April 2000. Dissolved data for 500m inventory were estimated from reported seawater profiles (Milne et al., 2010). The lateral component was estimated by taking the difference between input flux (wet and calculated dry) and output flux (trap). Positive values correspond to lateral flux flowing out of the box, whereas negative values correspond to lateral flux into the box.

Time period and res. depth	Residence time (d) [Filtered SW + May Suspended particles]						Estimated lateral component (nmol m^{-2} d^{-1})		
	Wet flux (soluble) + calculated dry flux (soluble)			Trap flux (500 m)					
	Fe	Mn	Zn	Fe	Mn	Zn	Fe	Mn	Zn
Jul- Sept (0-50m)	7.63	60.1	2.39	0.86	184	15.3	1200	393	4200
Oct-Dec (0-200m)	14.3	25.6	2.79	0.56	166	7.65	-14400	1360	3680
Jan-Apr (0-100m)	28.5	1.17	3.10	0.39	34.7	7.34	-37000	33800	3990
Jul-Apr (0-500m)	141	50.3	35.9	1.28	135	15.9	-73600	3250	311

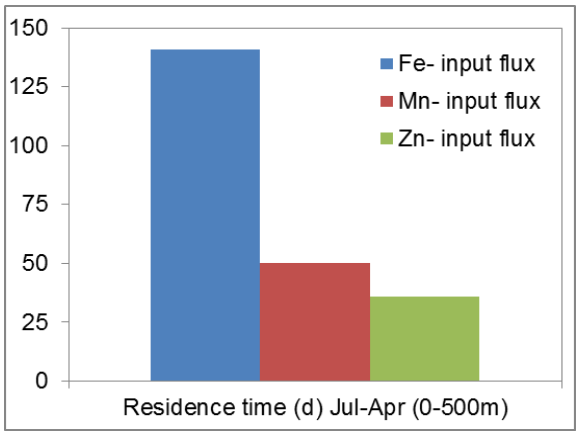

Figure 14 Residence time (d) for Fe, Mn and Zn for the entire sampling period (July – April 2000). Calculations considered total input flux (wet + calculated dry) and the total reservoir (dissolved + suspended particulate) from 0-500 m.

For instance, it has been reported that a high percentage of dissolved Fe in the surface waters is in the colloidal phase (Berquist et al., 2007). Organically bound Zn has been reported to dominate the dissolved fraction, thereby retaining Zn in solution (Bruland et al., 1991). Mn in surface waters undergoes extensive redox reactions, in which a surface maximum is observed in seawater concentration (Bruland et al., 1991).

2.3.6 Lithogenic and Biogenic Components

Calculations to determine the biogenic component of trap sediments and suspended particle material were modified from Frew et al, (2006). Instead of using crustal ratios reported in Wedepohl (1995), crustal ratios reported in Taylor and McLennan (1985) were used. The lithogenic component was first determined by multiplying the particulate Al [PAl] (assumed to be entirely lithogenic) by the crustal abundance ratio for a given

element. The biogenic component is the difference between the total particulate element, e.g. Total [PFe], and the calculated lithogenic value as shown below.

Total [PFe] = Lithogenic [PFe] + Biogenic [PFe]

The average lithogenic and biogenic components for Fe, Mn and Zn in each trap depth were determined and are reported as seasonal averages (Fig. 15a-c). For each element, lithogenic results are positively correlated between seasons (R^2=0.96 to R^2=0.98). Conversely less agreement was found between the biogenic components of all elements during each season. With depth, the biogenic component of Fe (Fig. 15a) decreases, as does Zn to a lesser degree (Fig. 15c). On the other hand the biogenic component of Mn generally increases with depth, but was at a maximum at 1500m during the January through April period (Fig. 15b). Fe was predominately lithogenic, with a maximum biogenic component observed in the 500 m trap. On the other hand, Zn was predominately biogenic at each depth. Mn was intermediate between the lithogenic and biogenic fractions at the 500 m trap, but like Zn, Mn was predominately biogenic in the mid and deep-water traps.

The composition of lithogenic and biogenic Fe, Mn and Zn in trap profiles illustrates the difference in processing that these elements undergo. A large contributing factor may be the loss of organic material in sediment traps as they are further processed with depth and the association of these elements to organic carbon (Huang and Conte, 2009). Lithogenic Fe appears to increase with depth which suggests the decomposition of the organic material in the sediment thereby decreasing the association of Fe to organic

carbon in addition to the possibility of scavenging laterally advected particles containing Fe. Zn behaves similarly in that the biogenic component decreases with depth. This is supported by the association with organic carbon in trap materials. The increase in the biogenic component of Mn with depth may be explained by the association with Mn oxides and small lithogenic particles with depth (Huang and Conte, 2009). We observe an increase in biogenic Mn with a decrease in biogenic Fe. This supports the Mn oxides coating the sediments scavenging redox sensitive elements, in this case, lithogenic Fe.

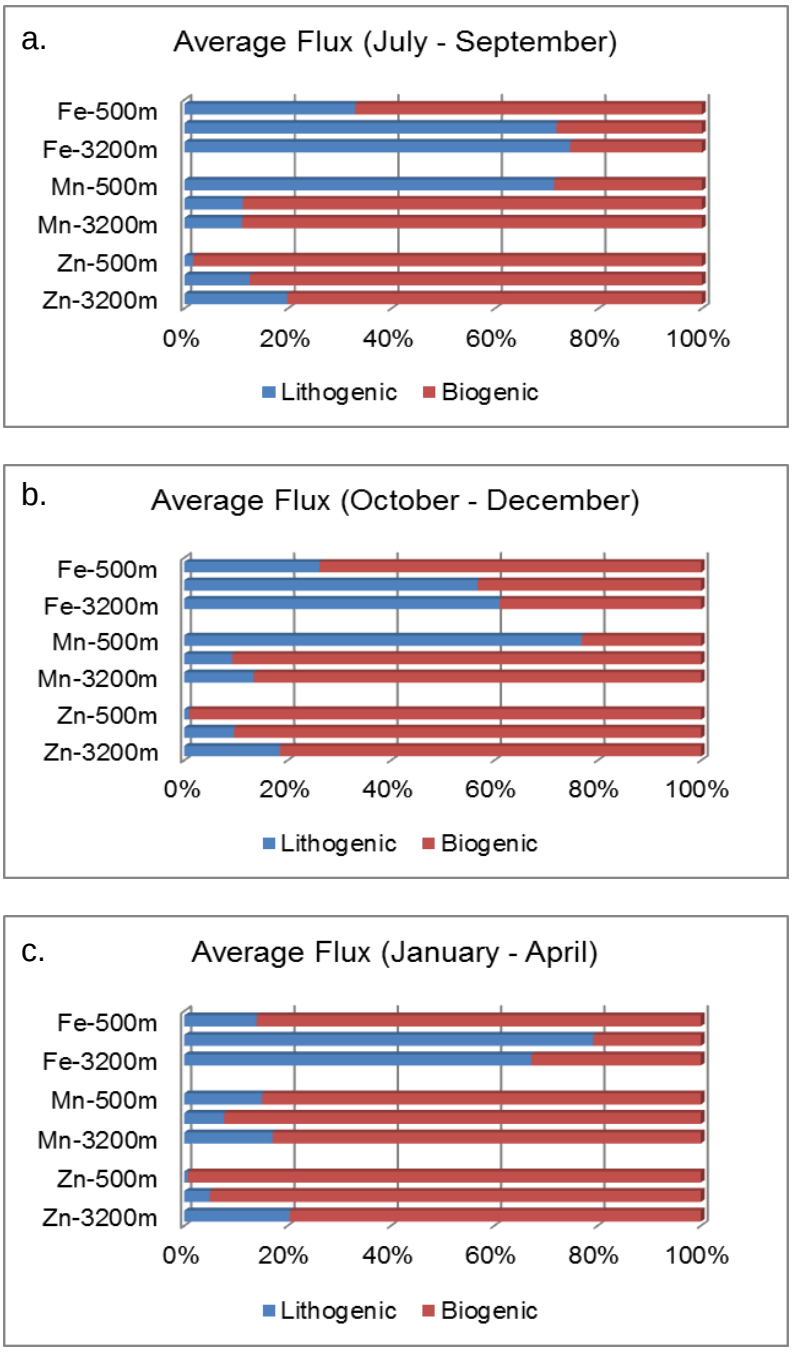

Figure 15. Seasonal lithogenic to biogenic composition (%) of trap sediments a) Jul. to Sept. b) Oct. to Dec. c) Jan. to Apr.

The average lithogenic and biogenic component was also calculated for the entire sampling period (Fig. 16). Similar trends were observed in the total average as for the seasonal averages; Fe was increasingly lithogenic with depth, Zn was increasingly lithogenic with depth and Mn was intermediate in favor the biogenic fraction. For comparison, annual averages were calculated from reported trap sediment data (Huang and Conte, 2005), that were collected from the same sampling site from January 2002 through March 2005 (Fig. 17). The lithogenic components for all elements from this investigation and the reported investigation were positively correlated, as shown in Figure 18. However, like the seasonal averages, the biogenic component did not show this relationship. In this case, there was no significant relationship between the biogenic components due to the Fe composition at 500 m.

Overall, we have found similar lithogenic trends between seasons and annual averages and variability in the biogenic component for the same timeframe, as observed in the 500 m trap. These results indicate the variable impact on trace metal distribution by biology, as well as the influence of atmospheric input. Lateral advection in the deep waters may also contribute to the conservative trends observed with depth.

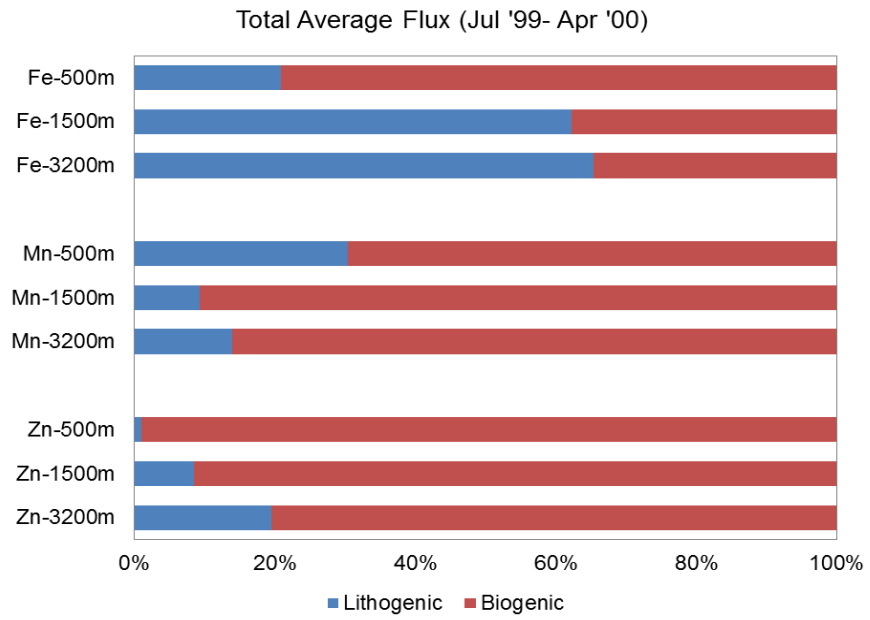

Figure 16. Average lithogenic to biogenic composition (%) of trap sediments for entire period

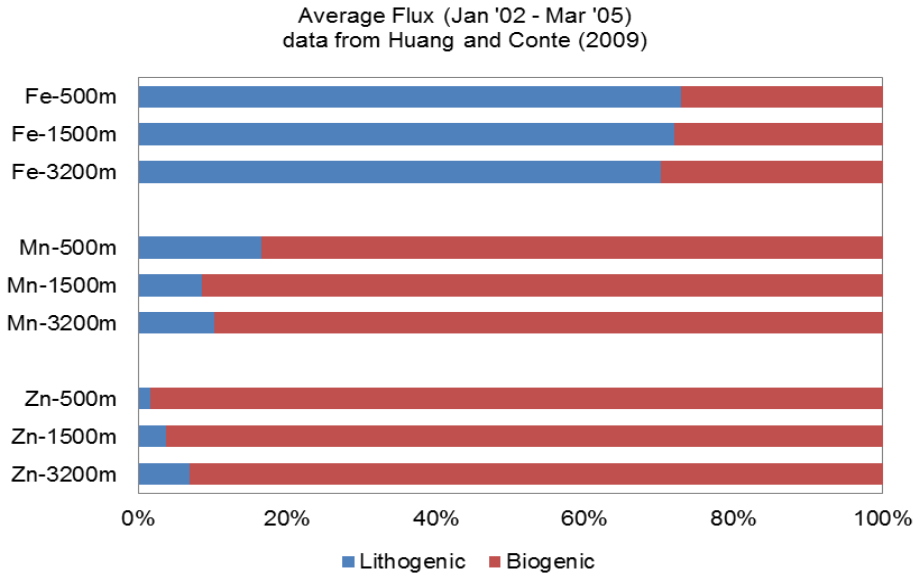

Figure 17. Average annual lithogenic to biogenic composition (%) of trap sediments calculated from literature trap data

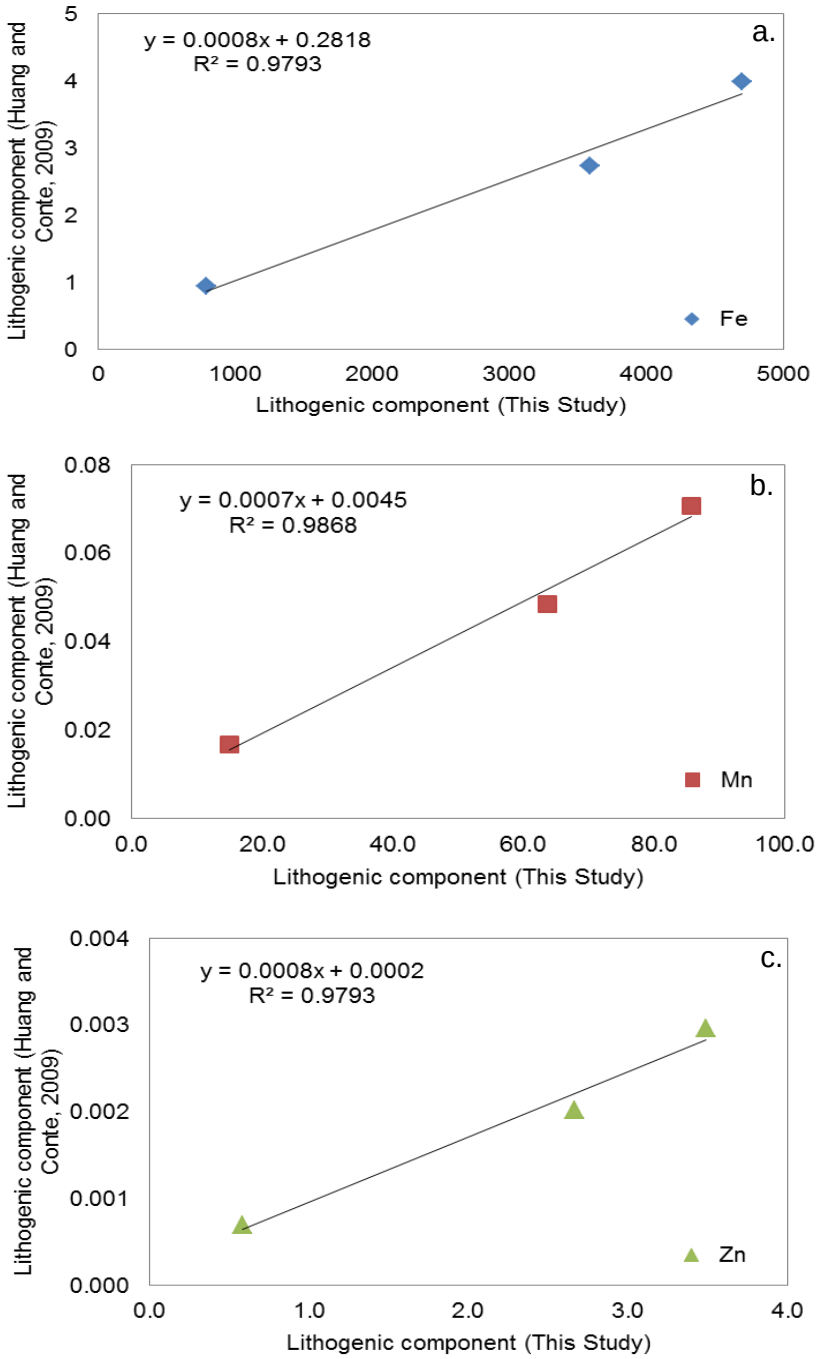

Figure 18. Positive correlation plots between the lithogenic component of a) Fe b) Mn and c) Zn in this study (x-axis) versus the lithogenic component calculated for trap averages reported in Huang and Conte (2009) (y-axis).

2.3.7 Stoichiometic Ratios

Sediment trap and suspended particles from McLane pumps can be directly compared if either the volume of water processed above the trap is determined or if the mass on the particles on the particle filter are. Although these parameters were not available, biogenic metal concentrations normalized with particulate organic carbon (POC) were used to compare both samples types. The composition of organic carbon in trap sediments and suspended particles were provided by Maureen Conte's lab at the Marine Biological Laboratory. Utilizing the calculated biogenic component values for trap sediments and suspended particles, biogenic element to organic carbon ratios were determined (Tables 10 and 11).

Average seasonal ratios were calculated in trap sediments as well as average ratios for the entire sampling season (Table 10). In addition, ratios were calculated from reported average sediment trap data from January 2002 to March 2005 (Huang and Conte, 2009). The organic carbon values between the two studies were surprisingly consistent. In the 500 m trap there was a percent difference of < 4%, and in the 1500m and 3200m traps the percent different was roughly 10%. With increasing trap depth, decreasing concentration of the organic carbon was observed. This trend is negatively correlated with the increasing concentration of Fe and Mn, but positively correlated with the increase of Zn with depth. These results are supported by observations reported in Huang and Conte (2009). Mid-water, there is a depletion of organic matter along with associated elements, including Zn. On the other hand, lithogenic elements, including Fe and Mn, increase with depth due to a suite of processes such as chemical scavenging and particle

aggregation. Additionally, lateral advection of lithogenic materials has been speculated to be the main supply of the increased lithogenic flux in the deep water.

Biogenic element to organic carbon ratios in suspended particles displays similarities as with the ratios in trap sediments (Table 11). With depth, the organic carbon decreases and is negatively correlated with the increase in Fe and Mn in ratios. Unlike the results in the sediment traps, Zn in suspended particles is also negatively correlated and the ratio increases with depth. This may be due to the processing of Zn and associated organic materials in traps with depth and increase in the suspended phase, intermediate to the dissolved phase. This result agrees with the remineralization that occurs with depth as historically observed in nutrient-like trace metal profiles.

Stoichiometric ratios have been reported for the composition for phytoplankton, however most recent studies have reported ratios normalized to P. Ratios of Fe, Mn and Zn normalized to carbon were reported for the composition of netted phytoplankton (Martin and Knauer, 1973). The stoichiometric ratio was as follows: $C_{1000}Fe_{0.05}Mn_{0.0037}Zn_{0.0079.}$ In the surface particles for January (20m) and May (50m), we observed ratios that were not only comparable to each other but also to the reported stoichiometric ratios (Fig. 19). We report a stoichiometric ratio in the surface suspended particles of $C_{1000}Fe_{0.10}Mn_{0.0035}Zn_{0.005}$. Particles with depth became more enriched in biogenic elements relative to organic carbon, suggesting the influence of abiotic factors such as aggregation.

Although the ratios in this investigation are highly enriched in Fe, this can be accounted for. Higher composition of Fe in suspended particles in comparison to plankton alone can be supported by the prevalence of colloidal Fe in the surface waters of the North Atlantic (Berquist et al., 2007). These colloids most likely were aggregated and collected on the particle filter along with plankton. Zn on the other hand was relatively deficient, which may be due to the remineralization of Zn from the particulate to the dissolved phase in the surface waters. In the process for collection, it is unavoidable to isolate biogenic particles which results in a composition that is weighted by abiogenic particles (Ho et al., 2007). Deduced from suspended particles, the stoichiometric ratios for phytoplankton can only be estimated but can be a useful tool indicative of biogenic processing of bioactive elements.

Table 10. Average biogenic metal to organic carbon ratios in sediment traps at 500m during three seasons. *Calculated from data reported in Huang and Conte (2009).

Period	OrgC (mmol/g)	Biogenic Fe :OrgC (µmol: mmol)	Biogenic Mn :OrgC (µmol: mmol)	Biogenic Zn :OrgC (µmol: mmol)
500m Trap				
Jul- Sept '99	0.33	4.2	0.01	0.09
Oct- Dec '99	0.16	17.4	0.03	0.47
Jan- Apr '00	0.38	10.6	0.17	0.17
AVG.	0.29	10.7	0.07	0.24
*Jan'02- Mar '05	0.28	1.2	0.30	0.14
1500m Trap				
Jul- Sept '99	0.27	4.2	1.5	0.06
Oct- Dec '99	0.16	33.5	7.7	0.31
Jan- Apr '00	0.31	1.2	1.3	0.09
AVG.	0.25	13.0	3.5	0.15
*Jan'02- Mar '05	0.22	4.88	2.4	0.24
3200m Trap				
Jul- Sept '99	0.20	7.1	2.9	0.06
Oct- Dec '99	0.11	42.0	7.7	0.22
Jan- Apr '00	0.22	5.8	1.3	0.04
AVG.	0.18	18.3	4.0	0.11
*Jan'02- Mar '05	0.16	10.7	3.9	0.25

Table 11. Biogenic metal to organic carbon ratios (µmol mol^{-1}) in suspended particles from McLane pumps with depth collected during January and May 2000.

Month, Year, Depth (m)	OrgC (mmol/L)	Biogenic Fe :OrgC (µmol: mmol)	Biogenic Mn :OrgC (µmol: mmol)	Biogenic Zn :OrgC (µmol: mmol)
Jan'00-20	0.00291	0.10	0.004	0.005
Jan'00-70	0.00174	0.87	0.124	-
Jan'00-120	0.00030	1.88	0.355	0.025
Jan'00-450	0.00023	3.92	1.830	0.031
Jan'00-3150	0.00007	7.39	2.300	0.113
May'00-50	0.00123	0.10	0.003	0.004
May'00-100	0.00081	0.09	0.117	0.005
May'00-550	0.00087	0.74	1.320	0.020
May'00-1550	0.00012	1.22	1.140	0.022
May'00-3250	0.00004	3.44	1.810	0.058

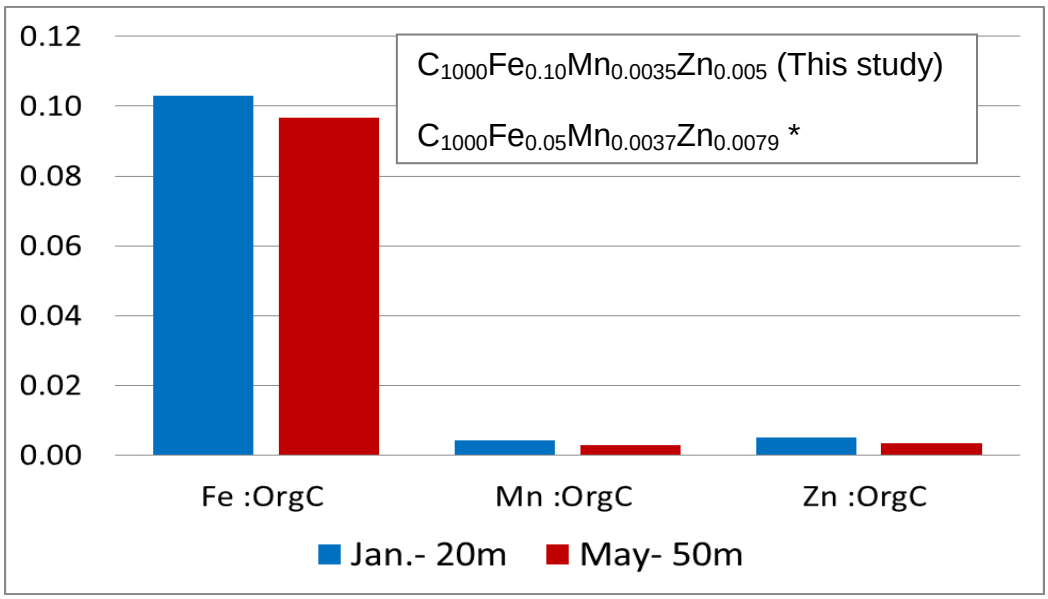

Figure 19. Biogenic element to organic carbon ratios for surface most particles collected during January 2000 and May 2000. The stoichiometric from this study represents an average between the two months. * Stoichiometric ratio for netted phytoplankton (Martin and Knauer, 1963).

2.4 Conclusion

We have shown the distribution of Fe, Mn and Zn in the water column in response to atmospheric deposition. Properties of these elements in trap sediments and suspended particles were calculated, including seasonal residence times comparing reservoirs as well as input and output flux, the lithogenic and biogenic component, crustal ratio, biogenic metal to organic carbon ratios and resulting stoichiometric ratios. These calculations were repeated using data reported in literature to make further comparisons and interpretations. We utilized complementary databases and records,

including air mass trajectories, CTD data, mass flux and observations in the sediment trap cup upon recovery to further interpret our results.

Seasonal input of bioactive trace metals in our sampling period were from three different sources, all of which may have influenced the solubility of the elements and consequently the bioavailability. Although the calculated dry deposition dominated the atmospheric input, the wet deposition was likely underestimated in the bulk sample. However we have shown that increased fluxes in the wet deposition were observed in the 500 m trap during August, December and April. August and April correspond to the highest periods of mass flux of the sampling seasons, whereas December corresponds to a low period of mass flux.

We attribute increased fluxes in the late summer into early fall to the rapid repackaging of atmospheric inputs, indicated by the high frequency of salp fecal pellets, as well as increased dust events during this period. The increasing mass flux with depth agrees with the highest frequency of salp fecal pellets observed in the deep water traps. Increased mixing in the water column during December most likely impacted the flux observed in the 500m trap. The input flux with the suspended particle reservoir could have aggregated upon mixing, became a part of the sinking flux and scavenged particles in transport from the surface waters. This process appears to agree with the suspended particle profiles for January. The increased mass flux as well as for all elements corresponds with the timing of the spring bloom in which grazing of the phytoplankton bloom would occur, transporting repackaged trace metals into the downward flux.

Residence times varied when comparing the input and output flux, considering the seasonal reservoirs. The longest range of residence times resulted when using input flux for calculations, however values for Fe were in agreement with literature values. Mn and Zn, on the other hand, had longer residence times when calculating residence time using output flux to the 500 m trap. Overall Fe, appears to have faster residence times in surface waters in comparison with deeper reservoirs, as supported in literature. Results reflect the influence of the advection component on the reservoir and, moreover, the residence time. Advection can include lateral advection of surface dusts as well as increased mixing, observed in the seasonal temperature profiles.

The biogenic component Fe, Mn and Zn in trap particles decrease for Fe and Zn, but increases for Mn. The lithogenic component of Fe appears to increase with depth, simultaneously as the biogenic Fe to organic carbon ratio increases. This can be explained by the association with Mn in the water column. The formation of Mn oxides on the trap particle surface would explain the increase in biogenic component, as well as the scavenging of lithogenic, redox sensitive elements. We attribute the decrease in the biogenic component of Zn to its association with organic carbon, which decreased with depth. However the biogenic Zn in suspended particles increases with depth as organic carbon decreases. Smaller suspended particles act as the intermediate phase between the large particles and the dissolved reservoir, thereby the decrease in biogenic Zn in trap sediments would result in an increase of the suspended fraction before becoming fully dissolved.

Overall this investigation supports the link between seasonal biotic and abiotic processing of trace metals and the interrelationship between the cycling of these elements. Furthermore analyzing synchronous samples across the partitioned phases highlights the processes involved in the exchange of trace metals between the particulate and the dissolved phases. In the future, this investigation could be extended to a suite of bioactive elements, such as Cu, Ni, Co, and Cr, essential for marine life. In this way, we would be able to observe the relationships between elements associated with particles as they are processed, beginning from atmospheric delivery to fate and transport in the open ocean.

Chapter 3

CAPSTONE

3.1 Atmospheric Samples and Sediment Traps

A compiled log of the initial procedures performed on the bulk and wet atmospheric as well as the trap samples would have been very valuable. Both samples types were previously digested by Zhenglong and colleagues and were analyzed for Al, Fe, Mn and Zn using GFAAS. One of the first tasks was to locate original digests from storage. Although the trap digests were recovered, the atmospheric digests were not, so we were limited by the atmospheric data that already existed. For the May trap samples, digests assumed to be original digests were found in other bottles than the original digests for the other recovery dates. However, upon analysis we found that these samples may have been dilutions. The concentrations calculated using absorbance readings from the GFAAS were roughly 100-fold larger than the concentrations calculated using the ICPMS. This prompted the use of a combination of the GFAAS and ICPMS data to check values and fill in the gaps where dilutions were suspected. If atmospheric samples could be recovered, it would provide for another check between the two instruments. Furthermore, reanalysis of the atmospheric data would be a way to directly add more elements to the discussion of this study. We have ICPMS data for a

suite of elements, including Mg, Ti, V, Cr, Mo, Mn, Fe, Co, Ni, Cu, Zn, Cd, and Al, available for trap and suspended particles.

3.2 Suspended Particles

For future investigations with suspended particle filters, there are several suggestions. First, it is suggested that further experimentation with the digestion procedure is conducted. We have initial GFAAS data for Al, Fe and Zn for the first replicate of the suspended particle filter digests, which we compared to the data from the ICPMS analysis. We observed that the samples of lower concentration had better agreement between the two methods, but there was a larger difference between samples of high concentration in which the ICPMS values were larger. Results suggest that there was incomplete digestion for several elements. Although the filters each went through two rounds of digestion, possibly the strength and combination of acids could be modified to make digestion more efficient. Complete digestion could be tested by checks with both instruments to see if there is agreement with samples of high concentrations relative to the sample set.

In addition, it is recommended using round bottom vials for digestions. The last replicate of suspended particle filters was digested using conical vials, in which the filter melted to the sides of the vial even while the vial was sealed. High temperatures for an extended amount of time appear to cause the Supor filter to change composition but not digest. The filter will either flake off into the digest or become a gum-like substance where it is in direct contact with the vial. Several labs are currently working on ways to optimize the digestion procedure for these filters, or may eventually decide to

use a different material all together. In this case it seems that future literature will have useful guidance on this.

There was a larger variability between the triplicate digests from each particle filter (ST DEV < 40% sample), including the field blank, than what was reported in Sherrell and Boyle (1992). One suggestion was mentioned by Dr. Church, after analysis of all replicates. By subsampling the filter in strips across the filter instead of in pie slices (how they were subsampled in this investigation), the aliquot is more likely able to represent the potential heterogeneity of the particle distribution on the surface. Considering the range in values for each sample, the resulting profiles agreed with reported profile trends and concentration ranges.

In regards to future work, it would be interesting to determine the contribution of the suspended particles to the downward flux from scavenging, as calculated in Sherrell and Boyle (1992). Although reported calculations were modeled to determine the contribution in the deep ocean, the use of different tracers could be used to extend this calculation to the mid and surface waters. Th-230 could be used for the 500 to 1500m interval, however, Th-234 and Po-210 would be better suited for surface studies. Currently a Po-210 profile is available for a time period that overlaps the sampling period for this investigation.

3.3 Seawater Samples

Unfiltered seawater data would account for the ‘total’ reservoir in the water column, from which the dissolved fraction could be estimated from the particle values. For this data to be collected, however, more time would be

required to optimize the extraction procedure using the equipment and materials available. Extensive recovery tests and blank checks of all solutions along with seawater standards would be necessary prior to the extraction of actual samples. Further investigation on the effect of using HNO_3 at lower strength with the Toyopearl resin would also be needed. The recommend procedure, from Milne et al. (2010), uses 10% HNO_3 to elute the elements off the column, whereas it is required to use only 1% HNO_3 during analysis for the ICPMS on campus. Although dilution of the sample is possible, the preconcentration larger volumes can result in matrix interferences if the ions from Group 1 and 2 of the periodic table are not removed. In addition, dilution may also result in ion counts beneath detection limits for the minor trace elements.

3.4 Analyses Using ICPMS

All samples, excluding seawater, were originally processed to be analyzed with GFAAS. Looking back at my data and the difference in comparison to GFAAS values, there are ways that I could have improved my eventual analyses with ICPMS. For instance, it would be beneficial to evaporate and re-digest all samples, bringing them back up to volume in 1% HNO_3. This would decrease the chance for incomplete digestion and also ensure the same matrices were uniform. Having to dilute each of my samples from the original 5% HNO_3 matrix, in addition to larger dilutions necessary for sediment traps, most likely caused my samples to be in a slightly different percentage of weak HNO_3. In addition they would have differed from the matrix of the standard solutions in 1% HNO_3. Overall, data for this

investigation could be improved by becoming more familiar with the limits of the instrumentation as well as becoming more experienced in how to interpret data for repeat runs, if necessary.

3.5 Reflection

This experience was certainly one of learning, how to work through instrument malfunctions, human error, incomplete instructions and misinterpretations, but it was the small successes that guided this research into new directions. Overall, my suggestion to a student that wishes to continue this investigation would be to initiate direct and regular contact with the labs that specialize in each facet of the project at hand. This way, it would be possible to see if published protocols have recently been improved upon. Furthermore regular discussion with peers that are performing similar research would be beneficial to expand current ideas and approaches to the work at hand. At times, even more beneficial are the questions from those outside of the field that require application to the bigger picture. These connections would provide sources of guidance and tips, to try to avoid mishaps and collect the best data possible to contribute to the growing knowledge of trace metal research.

REFERENCES

Achilles, K.M., Church, T.M., Wilhelm, S.W., Luther, G.W., Hutchins, D.A. 2003. Bioavailability of iron Trichodesmium colonies in the western subtropical Atlantic Ocean. Limnol. Oceanogr. 48, 2250-2255.

Andersen, N.G., Nielsen, T.G., Jakobsen, H.H., Munk, P., Riemann, L., 2011. Distribution and production of plankton communities in the subtropical convergence zone of the Sargasso Sea. II. Protozooplankton and copepods. Mar. Ecol. Prog. Ser. 426, 71-86.

Arimoto, R., Duce, R.A., Savoie, D.L., Prospero, J.M., 1992. Trace elements in aerosol particles from Bermuda and Barbados: Concentrations, sources and relationships to aerosol sulfate. J. Atmos. Chem. 14, 439-457.

Berquist, B. A., Wu, J., Boyle, E. A., 2007. Variability in oceanic dissolved iron is dominated by the colloidal fraction. Geochim. Cosmochim. Ac. 71, 2690-2974.

Bory, A., Dulac, F., Moulin, C., Chiapello, I., Newton, P.P., Guelle, W., Lambert, C.E., Bergametti, G., 2002. Atmospheric and oceanic dust fluxes in the northeastern tropical Atlantic Ocean: how close a coupling? Ann Geophys-Germany 20, 2067-2076.

Bruland, K.W., Donat, J.R., Hutchins, D.A., 1991. Interactive Influences of Bioactive Trace-Metals on Biological Production in Oceanic Waters. Limnol. Oceanogr. 36, 1555-1577.

Butler, A., 2005. Marine siderophores and microbial iron mobilization. Biometals 18, 369-374.

Chen, L.Q., Duce, R.A., 1983. The sources of sulfate, vanadium and mineral matter in aerosol-particles over Bermuda. Atmos. Environ. 17, 2055-2064.

Chester, R., Murphy, K.J.T., Lin, F.J., Berry, A.S., Bradshaw, G.A., Corcoran, P.A., 1993. Factors controlling the solubilities of trace metals from nonremote aerosols desposited to the sea-surface by the dry deposition mode. Mar. Chem. 42, 107-126.

Church, T. M., Jickells, T. D., 2010. Biogeochemical processes at the air/sea boundary. Chem. Rev. 1-69, in revision.

Church, T.M., Tramontano, J.M., Scudlark, J.R., Jickells, T., Tokos, J., J. J., Knap, A.H., Galloway, J., 1984. The wet deposition of trace metals to the western Atlantic Ocean at the mid-Atlantic coast and on Bermuda. Atmos. Environ. 18, 2657-2664.

Conte et al., unpublished salp data

Conte, M.H., Dickey, T.D., Weber, J.C., Johnson, R.J., Knap, A.H., 2003. Transient physical forcing of pulsed export of bioreactive material to the deep Sargasso Sea. Deep-Sea Res. Part I-Oceanogr. Res. Pap. 50, 1157-1187.

Conte, M.H., Ralph, N., Ross, E.H., 2001. Seasonal and interannual variability in deep ocean particle fluxes at the Oceanic Flux Program (OFP)/Bermuda Atlantic Time Series (BATS) site in the western Sargasso Sea near Bermuda. Deep-Sea Res. Part II-Top. Stud. Oceanogr. 48, 1471-1505.

Croot, P.L., Streu, P., Baker, A.R., 2004. Short residence time for iron in surface seawater impacted by atmospheric dry deposition from Saharan dust events. Geophys. Res. Lett. 31, -.

Desboeufs, K.V., Losno, R., Colin, J.L., 2001. Factors influencing aerosol solubility during cloud processes. Atmos. Environ. 35, 3529-3537.

Frew, R.D., Hutchins, D.A., Nodder, S., Sanudo-Wilhelmy, S., Tovar-Sanchez, A., Leblanc, K., Hare, C.E., Boyd, P.W., 2006. Particulate iron dynamics during FeCycle in subantarctic waters southeast of New Zealand. Glob. Biogeochem. Cycle 20, -.

Huang, S., Conte, M.H., 2009. Source/process apportionment of major and trace elements in sinking particles in the Sargasso sea. Geochim. Cosmochim. Ac. 73, 65-90.

Huang, S., Turekain, K.K., Rahn, K.A., Arimoto, R., Graustein, W.C., 1999. Semiannual cycles of pollution at Bermuda. J. Geophys. Res-Atmos 104, 30,309-330,317.

Hunter, K.A., Kim, J.P., Croot, P.L., 1997. Biological roles of trace metals in natural waters. Environ. Monit. Assess. 44, 103-147.

Ho, T-Y., Wen, L-S., You, C-F., Lee, D-C., 2007. The trace-metal composition of size fractionated plankton in the South China Sea: Biotic versus abiotic sources. Limnol. Oceanogr. 52, 1776-1788.

Jickells, T., 1995. Atmospheric Inputs of Metals and Nutrients to the Oceans - Their Magnitude and Effects. Mar. Chem. 48, 199-214.

Jickells, T.D., 1999. The inputs of dust derived elements to the Sargasso Sea; a synthesis. Mar. Chem. 68, 5-14.

Jickells, T.D., Knap, A.H., Church, T.M., 1984. Trace metals in Bermuda rainwater. J. Geophys. Res. 89, 1423-1428.

Kieber, R.J., Skrabal, S.A., Smith, B.J., Willey, J.D., 2005. Organic complexation of Fe(II) and its impact on the redox cycling of iron in rain. Environ. Sci. Technol. 39, 1576-1583.

Kadko, D., Prospero, J., 2011. Deposition of ^{7}Be to Bermuda and the regional ocean: Environmental factors affecting estimates of atmospheric flux to the ocean. J. Geophys. Res. 116, C02013, doi:10.1029/2010JC006629

Kim, G., Alleman, L.Y., Church, T.M., 1999. Atmospheric depositional fluxes of trace elements, Pb-210, and Be-7 to the Sargasso Sea. Glob. Biogeochem. Cycle 13, 1183-1192.

Kuss, J., Waniek, J.J., Kremling, K., Schulz-Bull, D.E., 2010. Seasonality of particle-associated trace element fluxes in the deep northeast Atlantic Ocean. Deep-Sea Res. Part I-Oceanogr. Res. Pap. 57, 785-796.

Lewis, B.L., Luther, G.W., Lane, H., Church, T.M., 1995. Determination of Metal-Organic Complexation in Natural-Waters by Swasv with Pseudopolarograms. Electroanal. 7, 166-177.

Lim, B., Jickells, T.D., Colin, J.L., Losno, R., 1994. Solubilities of Al, Pb, Cu, and Zn in Rain Sampled in the Marine-Environment over the North-Atlantic Ocean and Mediterranean-Sea. Glob. Biogeochem. Cycle 8, 349-362.

Lomas, M.W., Lipschultz, F., Nelson, D.M., Krause, J.W., Bates, N.R., 2009. Biogeochemical responses to late-winter storms in the Sargasso Sea, I-Pulses of primary and new production. Deep-Sea Res. Part I-Oceanogr. Res. Pap. 56, 843-860.

Maldonado, M. T., Allen, A. E., Chong, J. S., Lin, K., Leus, D., Karpenko, N., Harris, S. L. 2006. Copper-dependent iron transport in coastal and oceanic diatoms. Limnol. Oceanogr. 51, 1729-1743.

Martin, J.H., Coale, K.H., Johnson, K.S., Fitzwater, S.E., Gordon, R.M., Tanner, S.J., Hunter, C.N., Elrod, V.A., Nowicki, J.L., Coley, T.L., Barber, R.T., Lindley, S., Watson, A.J., Vanscoy, K., Law, C.S., Liddicoat, M.I., Ling, R., Stanton, T., Stockel, J., Collins, C., Anderson, A., Bidigare, R., Ondrusek, M., Latasa, M., Millero, F.J., Lee, K., Yao, W., Zhang, J.Z., Friederich, G., Sakamoto, C., Chavez, F., Buck, K., Kolber, Z., Greene, R., Falkowski, P., Chisholm, S.W., Hoge, F., Swift, R., Yungel, J., Turner, S., Nightingale, P., Hatton, A., Liss, P., Tindale, N.W., 1994. Testing the iron hypothesis in ecosystems of the equatorial Pacific Ocean. Nature 371, 123-129.

Martin, J. H., Knauer, G. A., 1973. The elemental composition of plankton. Geochim. Cosmochim. Ac. 37, 1693-1653.

Menzel, D.W., Ryther, J.H., 1960. The Annual Cycle of Primary Production in the Sargasso Sea Off Bermuda. Deep-Sea Res 6, 351-367.

Milne, A., Landing, W., Bizimis, M., Morton, P., 2010. Determination of Mn, Fe, Co, Ni, Cu, Zn, Cd and Pb in seawater using high resolution magnetic sector inductively coupled mass spectrometry (HR-ICP-MS). Anal. Chim. Acta 665, 200-207.

Moffett, J.W., Brand, L.E., 1996. Production of strong, extracellular Cu chelators by marine cyanobacteria in response to Cu stress. Limnol. Oceanogr. 41, 388-395

Morel, F.M.M., Price, N.M., 2003. The biogeochemical cycles of trace metals in the oceans. Science 300, 944-947.

Pohl, C., Loffler, A., Hennings, U., 2004. A sediment trap flux study for trace metals under seasonal aspects in the stratified Baltic Sea (Gotland Basin; 57 degrees 19.20 ' N; 20 degrees 03.00 ' E). Marine Chemistry 84, 143-160.

Santschi, P.H., 1984. Particle-flux and trace-metal residence time in natural-waters. Limnol. Oceanogr. 29, 1100-1108.

Sarthou, G., Baker, A.R., Blain, S., Achterberg, E.P., Boye, M., Bowie, A.R., Croot, P., Laan, P., de Baar, H.J., Jickells, T.D., Worsfold, P.J., 2003. Atmospheric iron deposition and sea-surface dissolved iron concentrations in the eastern Atlantic Ocean. Deep-Sea Res. Part I-Oceanogr. Res. Pap. 50, 1339-1352.

Sedwick, P.N., Church, T.M., Bowie, A.R., Marsay, C.M., Ussher, S.J., Achilles, K.M., Lethaby, P.J., Johnson, R.J., Sarin, M.M., McGillicuddy, D.J., 2005. Iron in the Sargasso Sea (Bermuda Atlantic Time-series Study region) during summer: Eolian imprint spatiotemporal variability, and ecological implications. Glob. Biogeochem. Cycle 19, GB4006.

Sedwick, P.N., Sholkovitz, E.R., Church, T.M., 2007. Impact of anthropogenic combustion emissions on the fractional solubility of aerosol iron: Evidence from the Sargasso Sea. Geochem. Geophy. Geosy. 8, -.

Sherrell, R.M., Boyle, E.A., 1992. The trace metal composition of suspended particles in the oceanic water colum near Bermuda. Earth Planet. Sci. Lett. 111, 155-174.

Shi, Z.B., Krom, M.D., Bonneville, S., Baker, A.R., Jickells, T.D., Benning, L.G., 2009. Formation of Iron Nanoparticles and Increase in Iron Reactivity in Mineral Dust during Simulated Cloud Processing. Environ. Sci. Technol. 43, 6592-6596.

Sholkovitz, E.R. et al., unpublished FeAST data

Steinberg, D.K., Carlson, C.A., Bates, N.R., Johnson, R.J., Michaels, A.F., Knap, A.H., 2001. Overview of the US JGOFS Bermuda Atlantic Time-series Study (BATS): a decade-scale look at ocean biology and biogeochemistry. Deep-Sea Res. Part II-Top. Stud. Oceanogr. 48, 1405-1447.

Taylor, S.R., McLennan, S.M., 1985. The continental crust: Its composition and evolution. Blackwell Scientific.

Tian, Z.L., Ollivier, P., Veron, A., Church, T.M., 2008. Atmospheric Fe deposition modes at Bermuda and the adjacent Sargasso sea. Geochem. Geophy. Geosy. 9, -.

Turner, J.T., 2002. Zooplankton fecal pellets, marine snow and sinking phytoplankton blooms. Aquat. Microb. Ecol. 27, 57-102.

Ueyama, R., Monger, B.C., 2005. Wind-induced modulation of seasonal phytoplankton blooms in the North Atlantic derived from satellite observations. Limnol. Oceanogr. 50, 1820-1829.

Vraspir, J.M., Butler, A., 2009. Chemistry of marine ligands and siderophores. Annu. Rev. Mar. Sci. 1, 43-63.

Wedepohl, K.H., 1995. The composition of the continental-crust. Geochim. Cosmochim. Ac. 59, 1217-1232.

Whitfield, M., 2001. Interactions between phytoplankton and trace metals in the ocean. Adv Mar Biol 41, 1-128.

Wolff, G.T., Church, T.M., Galloway, J.N., Knap, A.H., 1987. An examination of SO_x, NO_x and trace metal wash-out ratios over the western Atlantic Ocean. Atmos. Environ. 21, 2623-2628.

Wu, J.F., Boyle, E., Sunda, W., Wen, L.S., 2001. Soluble and colloidal iron in the olgotrophic North Atlantic and North Pacific. Science 293, 847-849.

Appendix I

ATMOSPHERIC DATA

Table I.A Measured bulk (wet + dry) and wet atmospheric data from the AEROCE sampling tower. Data for Al and Fe were published, but data for Mn and Zn were not included (Tian et al., 2008).

Sample dates	Measured Atmospheric Flux (nmol m^{-2} d^{-1})							
	Al (Bulk)	Al (Wet)	Fe (Bulk)	Fe (Wet)	Mn (Bulk)	Mn (Wet)	Zn (Bulk)	Zn (Wet)
7/5-8/2/99	4570	1610	1120	344.0	20.4	13.80	12.70	4.70
8/2-9/7/99	10900	2330	2450	630.0	70.2	27.30	222.0	27.10
9/7-9/28/99	39200	1530	11800	381.0	400.0	19.30	4180.0	17.00
9/28-10/25/99	21000	1290	6130	388.0	1210.0	18.90	3560.0	6.210
10/25-11/24/99	3550	256	689	79.8	184.0	4.36	153.0	8.64
11/24-12/20/99	22500	1540	1610	718.0	95.5	6.73	424.0	2.73
12/20-1/20/00	3490	244	1080	20.7	172.0	0.73	636.0	3.18
1/20-2/18/00	3260	730	814	177.0	11.6	11.60	15.2	29.20
2/18-3/14/00	9150	652	2340	260.0	1480.0	16.60	2580.0	27.70
3/14-4/14/00	6080	1330	1260	344.0	32900.0	20.40	1350.0	10.20

Table I.B Calculated dry (bulk – wet) atmospheric data from the AEROCE sampling tower. Data for Al and Fe were published, but data for Mn and Zn were not included (Tian et al., 2008).

Sampling dates	Calculated Dry Atmospheric Flux (nmol m^{-2} d^{-1})			
	Al	Fe	Mn	Zn
7/5-8/2/99	2960	776	6.55	8.03
8/2-9/7/99	8590	1820	42.90	194.00
9/7-9/28/99	37700	11400	381.00	4160.00
9/28-10/25/99	19700	5740	1200.00	3560.00
10/25-11/24/99	3290	609	180.00	145.00
11/24-12/20/99	21000	888	88.70	421.00
12/20-1/20/00	3250	1060	172.00	633.00
1/20-2/18/00	2530	637	-	-
2/18-3/14/00	8490	2080	1470.00	2550.00
3/14-4/14/00	4750	912	32900.00	1340.00

Appendix II

SEDIMENT TRAP DATA

Table II.A Mass flux and organic carbon flux in sediment traps and three depths through the sampling period.

Sample ID/ Date		Mass Flux (mg m^{-2} d^{-1})			OrgC Flux (mg m^{-2} d^{-1})		
		500m	1500m	3200m	500m	1500m	3200m
9/99-3	6/27-7/12/99	23.10	58.5	59.0	3.25	3.60	3.25
9/99-4	7/12-7/27/99	22.30	63.8	98.2	3.31	5.85	4.81
9/99-5	7/27-8/10/99	30.30	29.9	54.7	9.41	2.98	3.19
9/99-6	8/10-8/24/99	12.10	36.1	24.0	1.43	3.09	1.64
9/99-7	8/24-9/8/99	20.60	30.5	18.1	2.85	2.37	0.98
9/99-8	9/7/99-9/28/99	11.80	29.1	48.1	n.a.	2.69	2.34
1/00-1	9/26-9/28/99	21.80	18.6	15.3	3.30	1.27	0.76
1/00-2	10/10-10/25/99	15.30	31.5	34.2	2.42	1.74	1.56
1/00-3	10/25-11/10/99	8.24	36.9	26.8	1.79	1.89	1.20
1/00-4	11/10-11/25/99	7.36	30.3	25.7	0.84	1.53	1.15
1/00-5	11/25-12/10/99	7.17	52.1	35.0	1.12	2.57	1.52
1/00-6	12/10-12/25/99	11.40	29.7	24.8	3.49	1.65	1.22
1/00-7	12/25-1/10/00	23.70	39.7	26.6	1.99	2.24	1.32
5/00-1	1/10-1/25/00	18.60	15.0	15.5	1.55	0.97	0.88
5/00-2	1/25-2/9/00	54.40	33.2	29.2	5.09	2.61	1.59
5/00-3	2/9-2/23/00	73.50	59.6	71.4	6.36	4.71	4.66
5/00-4	2/23-3/9/00	57.90	58.6	46.3	5.21	5.91	2.39
5/00-5	3/9-3/23/00	71.70	54.5	59.9	6.73	5.61	3.45
5/00-6	3/23-4/6/00	42.30	57.9	61.2	4.85	3.48	3.29
5/00-7	4/6-4/20/00	26.40	36.8	44.2	2.53	2.35	1.90

Table II.B Mass flux and organic carbon flux in sediment traps and three depths through the sampling period.

Sampling dates	Total-Al Trap Flux ($nmol\ m^{-2}\ d^{-1}$)			Total - Fe Trap Flux ($nmol\ m^{-2}\ d^{-1}$)		
	500m	1500m	3200 m	500m	1500m	3200 m
7/5-8/2/99	5000	26900	46800	1880	6740	13400
8/2-9/7/99	8140	40600	47500	9630	11800	14050
9/7-9/28/99	9550	30400	47700	2670	9520	11900
9/28-10/25/99	12800	81900	85100	2570	27600	31900
10/25-11/24/99	6230	66500	71300	1410	23300	23100
11/24-12/20/99	9970	57800	59000	18900	24000	17700
12/20-1/20/00	6260	15600	23700	1680	3790	6770
1/20-2/18/00	7680	23400	48700	13900	5940	14000
2/18-3/14/00	10300	27400	54000	13400	6880	15300
3/14-4/14/00	4580	12700	18000	13500	2650	4720

Table II.C Trap flux for Al and Fe in trap sediments at 500m, 1500m and 3200m.

Sample Date	Al fluxes (nmol m^{-2} d^{-1})			Fe fluxes (nmol m^{-2} d^{-1})		
	500m	1500m	3200m	500m	1500m	3200m
6/27-7/12/99	1800	13300	27300	493	3630	7740
7/12-7/27/99	3210	13600	19540	1390	3110	5620
7/27-8/10/99	3550	15600	29600	1470	4320	8640
8/10-8/24/99	2120	15600	7430	3930	4630	2270
8/24-9/8/99	2470	9450	10400	4230	2840	3140
9/7/99-9/28/99	600	14200	22700	860	4420	4300
9/26-9/28/99	8950	16300	25000	1810	5100	7570
10/10-0/25/9	8180	23200	38500	1700	5920	10700
10/25-/10/99	4650	58700	46700	869	21700	21200
11/10-1/25/9	4050	21700	25100	978	6680	8680
11/25-/10/99	2180	44800	46100	431	16600	14400
12/10-/25/99	6460	22300	38100	3020	8840	11500
12/25-/10/00	3510	35600	21000	15900	15100	6240
1/10-1/25/00	1310	5970	8110	461	1820	2210
1/25-2/9/00	4940	9610	15600	1210	1980	4560
2/9-2/23/00	6810	11500	25200	5640	3110	7400
2/23-3/9/00	870	11900	23500	8290	2830	6600
3/9-3/23/00	7480	13300	26700	5510	3440	7540
3/23-4/6/00	2840	14100	27200	7930	3440	7700
4/6-4/20/00	2390	10900	16500	8070	2650	4720
4/20-5/3/00	n.a.	1060	803	n.a.	n.a.	n.a.
5/3-5/17/00	2190	740	722	5430	n.a.	n.a.

Table II.D Total trap flux for Mn and Zn corresponding to atmospheric sampling period.

Sampling dates	Total- Mn Trap Flux ($nmol\ m^{-2}\ d^{-1}$)			Total- Zn Trap Flux ($nmol\ m^{-2}\ d^{-1}$)		
	500m	1500m	3200 m	500m	1500m	3200 m
7/5-8/2/99	38.90	549	1440	28.8	30.9	32.8
8/2-9/7/99	51.80	1370	1100	111.0	40.4	19.8
9/7-9/28/99	6.32	1270	840	72.0	47.4	56.7
9/28-10/25/99	7.03	3370	1770	84.2	84.9	56.5
10/25-11/24/99	21.50	2600	2330	116.0	75.4	55.5
11/24-12/20/99	110.00	2190	1770	258.0	167.0	65.9
12/20-1/20/00	113.00	869	699	66.5	67.0	28.2
1/20-2/18/00	128.00	1120	790	71.9	90.6	38.2
2/18-3/14/00	97.20	649	600	79.9	17.8	20.3
3/14-4/14/00	363.00	1120	1000	384.0	70.5	21.3

Table II.E Trap flux for Mn and Zn at 500 m, 1500 m and 3200 m.

Sample ID/ Date		Mn fluxes (nmol m^{-2} d^{-1})			Zn fluxes (nmol m^{-2} d^{-1})		
		500m	1500m	3200m	500m	1500m	3200m
9/99-3	6/27-7/12/99	29.60	489.0	830	8.89	18.80	15.10
9/99-4	7/12-7/27/99	9.22	59.30	609	19.90	12.10	17.70
9/99-5	7/27-8/10/99	160.00	467.0	876	33.10	9.90	7.72
9/99-6	8/10-8/24/99	n.a.	499.0	222	12.40	27.90	6.19
9/99-7	8/24-9/8/99	35.80	399.0	n.a.	65.10	2.66	5.88
9/99-8	9/7/99-9/28/99	n.a.	547.0	n.a.	30.90	7.26	31.60
1/00-1	9/26-9/28/99	6.32	724.0	840	41.00	40.10	25.10
1/00-2	10/10-10/25/99	5.13	1110.0	1270	33.90	48.00	29.30
1/00-3	10/25-11/10/99	1.90	2260.0	502	50.30	36.90	27.20
1/00-4	11/10-11/25/99	21.10	916.0	823	28.90	30.10	22.30
1/00-5	11/25-12/10/99	0.41	1690.0	1510	87.00	45.30	33.20
1/00-6	12/10-12/25/99	9.53	974.0	1130	238.00	55.60	26.20
1/00-7	12/25-1/10/00	100.00	1220.0	640	19.60	111.00	39.70
5/00-1	1/10-1/25/00	29.50	324.0	401	46.40	12.50	12.80
5/00-2	1/25-2/9/00	83.80	545.0	298	20.10	54.50	15.40
5/00-3	2/9-2/23/00	79.10	578.0	403	39.10	48.60	21.30
5/00-4	2/23-3/9/00	48.70	544.0	387	32.80	42.00	16.90
5/00-5	3/9-3/23/00	81.90	332.0	264	50.10	11.10	10.70
5/00-6	3/23-4/6/00	15.40	317.0	336	29.80	6.77	9.57
5/00-7	4/6-4/20/00	17.70	365.0	310	35.00	14.30	2.62
5/00-8	4/20-5/3/00	n.a.	440.0	351	n.a.	32.80	6.71
5/00-9	5/3-5/17/00	345.00	318.0	346	349.00	23.40	11.90

Table II.F Calculated lithogenic and biogenic components of Fe in trap sediments at 500 m, 1500 m and 3200 m.

Sample ID	Lithogenic [TrapFe], (nmol m^{-2} d^{-1})			Biogenic [TrapFe], (nmol m^{-2} d^{-1})		
	500m	1500m	3200m	500m	1500m	3200m
9/99-3	370	2740	5620	123.0	892	2120
9/99-4	661	2790	4030	727.0	313	1600
9/99-5	731	3210	6090	738.0	1110	2550
9/99-6	436	3210	1530	3490.0	1430	735
9/99-7	509	1950	2150	3720.0	896	989
9/99-8	124	2920	4690	736.0	1510	-386
1/00-1	1850	3360	5140	-31.1	1740	2420
1/00-2	1690	4780	7920	18.4	1150	2730
1/00-3	959	12100	9610	-90.0	9560	11600
1/00-4	835	4470	5180	143.0	2220	3500
1/00-5	449	9230	9500	-18.4	7400	4930
1/00-6	1330	4580	7840	169032	4260	3640
1/00-7	723	7320	4320	15100.0	7790	1920
5/00-1	271	1230	1670	191.0	589	540
5/00-2	1020	1980	3210	197.0	-2.55	1350
5/00-3	1400	2360	5200	4230.0	745	2210
5/00-4	179	2460	4840	8110.0	373	1760
5/00-5	1540	2750	5510	3970.0	692	2040
5/00-6	586	2910	5610	7340.0	532	2100
5/00-7	491	2240	3400	7580.0	406	1320
5/00-8	n.a.	218	165	n.a.	n.a.	n.a.
5/00-9	452	152	149	4980.0	n.a.	n.a.

Table II.G Calculated lithogenic and biogenic components of Mn in trap sediments.

Sample ID	Lithogenic [TrapMn], (nmol m^{-2} d^{-1})			Biogenic [TrapMn], (nmol m^{-2} d^{-1})		
	500m	1500m	3200m	500m	1500m	3200m
9/99-3	6.57	48.7	99.8	23.1	440	730
9/99-4	11.7	49.6	71.5	-2.52	9.72	538
9/99-5	13.0	57.0	108	2.96	410	767
9/99-6	n.a.	57.0	27.2	n.a.	442	195
9/99-7	9.04	34.6	n.a.	26.8	365	n.a.
9/99-8	n.a.	51.8	n.a.	n.a.	495	n.a.
1/00-1	32.8	59.6	91.4	-26.5	664	749
1/00-2	29.9	84.8	141	-24.8	1029	1132
1/00-3	17.0	215	171	-15.1	2046	331
1/00-4	14.8	79.3	92.0	6.28	837	731
1/00-5	7.99	164	169	-7.58	1524	1343
1/00-6	23.6	81.4	139	-14.1	892	993
1/00-7	12.8	130	76.7	87.2	1086	563
5/00-1	4.81	21.8	29.7	24.7	302	371
5/00-2	18.1	35.2	57.1	65.7	510	241
5/00-3	24.9	41.9	92.3	54.1	536	311
5/00-4	3.18	43.7	85.9	45.5	500	301
5/00-5	27.4	48.8	97.9	54.5	283	166
5/00-6	10.4	51.6	99.6	4.94	266	236
5/00-7	8.73	39.9	60.5	9.01	325	250
5/00-8	n.a.	3.87	2.94	n.a.	436	348
5/00-9	8.03	2.71	2.64	337	315	343

Table II.H Calculated lithogenic and biogenic components of Zn in trap sediments.

Sample ID	Lithogenic [TrapZn], (nmol m^{-2} d^{-1})			Biogenic [TrapZn], (nmol m^{-2} d^{-1})		
	500m	1500m	3200m	500m	1500m	3200m
9/99-3	0.275	2.040	4.170	8.62	16.80	11.000
9/99-4	0.491	2.070	2.990	19.40	10.00	14.700
9/99-5	0.543	2.380	4.530	32.60	7.51	3.200
9/99-6	0.324	2.380	1.140	12.10	25.50	5.060
9/99-7	0.378	1.450	1.600	64.70	1.22	4.290
9/99-8	0.092	2.170	3.480	30.80	5.09	28.100
1/00-1	1.370	2.490	3.820	39.70	37.60	21.300
1/00-2	1.250	3.550	5.880	32.70	44.50	23.400
1/00-3	0.712	8.980	7.140	49.60	27.90	20.100
1/00-4	0.620	3.320	3.850	28.30	26.70	18.500
1/00-5	0.334	6.850	7.060	86.60	38.50	26.100
1/00-6	0.988	3.400	5.820	237.00	52.20	20.400
1/00-7	0.537	5.430	3.210	19.00	106.00	36.500
5/00-1	0.201	0.913	1.240	46.20	11.60	11.600
5/00-2	0.756	1.470	2.390	19.40	53.00	13.000
5/00-3	1.040	1.750	3.860	38.00	46.80	17.400
5/00-4	0.133	1.830	3.590	32.60	40.10	13.400
5/00-5	1.140	2.040	4.090	49.00	9.04	6.630
5/00-6	0.435	2.160	4.170	29.30	4.61	5.400
5/00-7	0.365	1.670	2.530	34.60	12.60	0.088
5/00-8	-	0.162	0.123	-	32.60	6.590
5/00-9	0.336	0.113	0.110	349.00	23.30	11.80

Table II.I Molar enrichment ratios to Al for Fe, Mn and Zn in sediment traps.

Sample ID	Fe Enrichment (Fe/Al)/0.206			Mn Enrichment (Mn/Al)/0.00366			Zn Enrichment (Zn/Al)/0.000153		
	500 m	1500 m	3200 m	500 m	1500 m	3200 m	500 m	1500 m	3200 m
9/99-3	1.33	1.33	1.38	4.51	10.00	8.31	32.4	9.24	1.49
9/99-4	2.10	1.11	1.40	0.79	1.20	8.52	40.6	5.81	2.43
9/99-5	2.01	1.35	1.42	1.23	8.20	8.09	61.0	4.15	0.70
9/99-6	9.00	1.44	1.48	n.a.	8.76	8.17	38.2	11.70	2.23
9/99-7	8.31	1.46	1.46	3.96	11.50	n.a.	172.0	1.84	1.51
9/99-8	6.96	1.52	0.92	n.a.	10.60	n.a.	337.0	3.35	3.72
1/00-1	0.98	1.52	1.47	0.19	12.10	9.20	30.0	16.1	2.70
1/00-2	1.01	1.24	1.34	0.17	13.10	9.04	27.1	13.5	2.04
1/00-3	0.91	1.79	2.21	0.11	10.50	2.94	70.7	4.10	1.56
1/00-4	1.17	1.50	1.67	1.42	11.50	8.94	46.7	9.06	2.38
1/00-5	0.96	1.80	1.52	0.05	10.30	8.96	261.0	6.61	1.93
1/00-6	2.27	1.93	1.46	0.40	12.00	8.13	241.0	16.30	1.84
1/00-7	21.90	2.07	1.44	7.79	9.360	8.34	36.4	20.50	5.08
5/00-1	1.70	1.48	1.32	6.14	14.80	13.50	231.0	13.70	4.23
5/00-2	1.19	1.00	1.42	4.63	15.50	5.22	26.6	37.00	2.65
5/00-3	4.02	1.32	1.42	3.17	13.80	4.37	37.5	27.70	2.26
5/00-4	46.20	1.15	1.36	15.3	12.40	4.50	246.0	23.00	1.93
5/00-5	3.57	1.25	1.37	2.99	6.81	2.70	43.8	5.43	1.07
5/00-6	13.50	1.18	1.37	1.47	6.14	3.37	68.4	3.13	0.94
5/00-7	16.40	1.18	1.39	2.03	9.15	5.13	95.9	8.55	0.42
5/00-8	n.a.	n.a.	n.a.	n.a.	114.00	119.00	n.a.	203.00	22.40
5/00-9	12.00	n.a.	n.a.	43.00	118.00	131.00	1040.0	207.00	44.30

Appendix III

SUSPENDED PARTICLE DATA

Table III.A Concentration of Al, Fe, Mn and Zn in suspended particles with flow meter data. *BDL refers to data that was below detection limit.

Sample Date and Depth	Al (nM)	Fe (nM)	Mn (nM)	Zn (nM)	Flow Meter Volume (L)
Jan-20 m	0.08	0.14	0.01	0.006	291.5
Jan-70 m	0.89	0.88	0.10	-	37.9
Jan-120 m	1.10	1.87	0.31	0.022	64.4
Jan-450 m	2.48	0.98	0.23	0.004	734.4
Jan-3150 m	2.60	0.81	0.10	0.005	451.9
May- 50 m	5.26	1.36	0.03	0.011	53.75
May-100 m	0.80	0.33	0.21	0.010	227.48
May-550 m	0.92	0.41	0.40	0.006	617
May-1550 m	2.68	0.84	0.28	0.006	1162
May-3250 m	4.19	1.12	0.15	0.005	1449.66
ST. Dev. Factor of the avg.	0.4	0.4	0.2	0.5	
Procedural Blank- % sample	2.6%	7.4%	BDL	BDL	
Filter Blank- % of sample	36%	71%	10%	24%	

Table III.B Lithogenic and biogenic Fe components in suspended particles.

Sample	[PFe] nM	[PAl] nM	Lith. [PFe], nM	Bio. [PFe], nM	% Lith.
Jan-20 m	0.144	0.081	0.017	0.127	12
Jan-70 m	0.884	0.893	0.184	0.700	21
Jan-120 m	1.870	1.100	0.227	1.640	12
Jan-450 m	0.981	2.480	0.511	0.471	52
Jan-3150 m	0.813	2.600	0.535	0.277	66
May- 50 m	1.360	5.260	1.080	0.281	79
May-100 m	0.330	0.799	0.165	0.165	50
May-550 m	0.410	0.921	0.190	0.220	46
May-1550 m	0.840	2.68	0.552	0.286	66
May-3250 m	0.116	4.190	0.863	0.252	77

Table III.C Lithogenic and biogenic Mn components in suspended particles.

Sample	[PMn] nM	[PAl] nM	Lith. [PMn], nM	Bio. [PMn], nM	% Lith.
Jan- 20 m	0.005	0.081	0.0003	0.005	5.5
Jan-70 m	0.103	0.893	0.0033	0.100	3.2
Jan-120 m	0.315	1.10	0.0040	0.311	1.3
Jan-450 m	0.228	2.48	0.0091	0.219	4.0
Jan-3150 m	0.096	2.60	0.0095	0.086	9.9
May- 50 m	0.028	5.26	0.0192	0.009	69
May-100 m	0.206	0.799	0.0029	0.203	1.4
May-550 m	0.399	0.921	0.0034	0.395	0.8
May-1550 m	0.276	2.68	0.0098	0.266	3.6
May-3250 m	0.148	4.19	0.0153	0.133	10

Table III.D Lithogenic and biogenic Zn components in suspended particles.

Sample	[PZn] nM	[PAl] nM	Lith. [PZn], nM	Bio. [PZn], nM	% Lith.
Jan-20 m	0.006	0.081	0.00001	0.006	0.2
Jan-70 m	-	0.893	-	-	-
Jan-120 m	0.022	1.10	0.0002	0.022	0.8
Jan-450 m	0.004	2.48	0.0004	0.004	9.2
Jan-3150 m	0.005	2.60	0.0004	0.004	8.6
May-50 m	0.011	5.26	0.0008	0.010	7.3
May-100 m	0.010	0.799	0.0001	0.010	1.3
May-550 m	0.006	0.921	0.0001	0.006	2.3
May-550 m	0.006	2.68	0.0004	0.005	7.5
May-250 m	0.005	4.19	0.0006	0.004	13

Appendix IV

DATA FOR RESIDENCE TIME CALCULATIONS

Table IV.A Seasonal input and output fluxes with corresponding dissolved and suspended particle reservoir data.

Date and Depth	Element	Average Flux ($nmol\ m^{-2}\ d^{-1}$)			Reservoir Size ($nmol/m^2$)		
		Trap (output)	Wet (input)	Dry (input)	Dissolved	Particles (May)	Particles (Jan)
Jul-Sept (0-50m)	Fe	4730.0	451.00	4670	20.8	68.20	28.60
	Mn	32.3	20.10	143	84.9	1.40	2.82
	Zn	70.5	16.30	1460	35.8	0.55	0.29
Jan-Apr (0-100m)	Fe	10600.0	200.0	1170	32.3	111.00	97.40
	Mn	175.0	12.30	8620	203	7.25	13.30
	Zn	151.0	17.60	1510	37.0	1.06	0.83
Jan-Apr (0-200m)	Fe	7620.0	395.00	2410	42.5	111.00	97.40
	Mn	46.0	10.00	488	270.0	7.25	13.30
	Zn	153.0	5.86	1370	41.1	1.06	0.83

Table IV.B Values estimated from filtered seawater profiles reported in Milne et al. (2010).

Depth (m^3/m^2)	Fe conc. (nM)
0	-
25	0.450
50	0.313
87.5	0.125
125	0.050
137.5	0.0563
200	0.250
250	0.275
500	0.313
600	0.417
700	0.596
1000	0.750
-	-

Depth (m^3/m^2)	Mn conc. (nM)
0	-
25	1.690
50	1.730
87.5	1.510
125	1.520
137.5	1.250
200	0.338
250	0.225
350	0.250
500	0.181
600	0.175
700	0.200
1000	0.338

Depth (m^3/m^2)	Zn conc. (nM)
0	-
22	0.140
55.55	0.055
77.77	0.022
111.1	0.001
200	0.091
350	0.147
500	0.389
600	0.642
700	0.905
1000	1.390
1150	1.510
-	-

Table IV.C Seasonal residence times calculated for Fe, Mn and Zn for dissolved and particulate reservoirs, using input and output flux data.

Residence Time (d)	Jul- Sept (0-50m)			Oct-Dec (0-200m)			Jan-Apr (0-100m)		
	Fe	Mn	Zn	Fe	Mn	Zn	Fe	Mn	Zn
Trap flux (output)									
Dissolved	0.13	74.40	14.40	0.16	161.94	7.46	0.001	0.29	0.06
Particulate (Jan)	0.17	2.47	0.12	0.35	7.97	0.15	0.29	0.02	0.001
Particulate (May)	0.41	1.22	0.22	0.40	4.36	0.19	0.06	0.01	0.002
Soluble wet + Soluble calculated dry (input)									
Dissolved	1.73	58.02	2.32	3.97	24.92	2.72	6.46	1.13	3.02
Particulate (Jan)	5.20	3.80	0.05	9.09	1.23	0.06	19.5	0.07	0.07
Particulate (May)	5.90	2.08	0.07	10.3	0.67	0.07	22.1	0.04	0.09

Table IV.D Residence times calculated for Fe, Mn and Zn over the entire sampling period from 0-500 m.

Residence Time (d)	Jul-Apr (0-500m)		
	Fe	Mn	Zn
Trap flux (output)			
Dissolved	0.461	103.	15.1
Particulate (Jan)	0.007	0.11	0.004
Particulate (May)	0.003	0.11	0.003
Soluble wet + Soluble calculated dry (input)			
Dissolved	50.5	38.4	34.0
Particulate (Jan)	90.1	11.9	1.83
Particulate (May)	221.	11.6	2.57